Pharmacol **79**(4): 735-741, 2011.
46) Hisaoka M, Matsuyama A, Nagao Y, *et al*: Identification of altered MicroRNA expression patterns in synovial sarcoma. *Genes Chromosomes Cancer* **50**(3): 137-145, 2011.
47) Subramanian S, Thayanithy V, West RB, *et al*: Genome-wide transcriptome analyses reveal p53 inactivation mediated loss of miR-34a expression in malignant peripheral nerve sheath tumours. *J Pathol* **220**(1): 58-70, 2010.
48) Itani S, Kunisada T, Morimoto Y, *et al*: MicroRNA-21 correlates with tumorigenesis in malignant peripheral nerve sheath tumor (MPNST) via programmed cell death protein 4 (PDCD4). *J Cancer Res Clin Oncol* **138**(9): 1501-1509, 2012.
49) Chai G, Liu N, Ma J, *et al*: MicroRNA-10b regulates tumorigenesis in neurofibromatosis type 1. *Cancer Sci* **101**(9): 1997-2004, 2010.
50) Gong M, Ma J, Li M, *et al*: MicroRNA-204 critically regulates carcinogenesis in malignant peripheral nerve sheath tumors. *Neuro Oncol* **14**(8): 1007-1017, 2012.
51) Greither T, Würl P, Grochola L, *et al*: Expression of microRNA 210 associates with poor survival and age of tumor onset of soft-tissue sarcoma patients. *Int J Cancer* **130**(5): 1230-1235, 2011.
52) 尾崎充彦，落谷孝広:【RNA医学・医療　あらたな診断・治療を拓く】RNAを利用する新しい医薬・医療 microRNA医薬によるがん治療への展開　がん転移モデルに対するmiRNAの核酸医薬としての検証を中心に. 医のあゆみ　**238**(5): 524-528, 2011.
53) Gandellini P, Profumo V, Folini M, *et al*: MicroRNAs as new therapeutic targets and tools in cancer. *Expert Opin Ther Targets* **15**(3): 265-279, 2011.
54) Lanford RE, Hildebrandt-Eriksen ES, Petri A, *et al*: Therapeutic silencing of microRNA-122 in primates with chronic hepatitis C virus infection. *Science* **327**(5962): 198-201, 2010.
55) Li W and Szoka FC Jr: Lipid-based nanoparticles for nucleic acid delivery. *Pharm Res* **24**(3): 438-449, 2007.
56) Kumar P, Wu H, McBride JL, *et al*: Transvascular delivery of small interfering RNA to the central nervous system. *Nature* **448**(7149): 39-43, 2007.
57) Ochiya T, Takahama Y, Nagahara S, *et al*: New delivery system for plasmid DNA in vivo using atelocollagen as a carrier material: the Minipellet. *Nat Med* **5**(6): 707-710, 1999.
58) Yamamoto Y, Kosaka N, Tanaka M, *et al*: MicroRNA-500 as a potential diagnostic marker for hepatocellular carcinoma. *Biomarkers* **14**(7): 529-538, 2009.
59) Ohyashiki K, Umezu T, Yoshizawa S, *et al*: Clinical impact of down-regulated plasma miR-92a levels in non-Hodgkin's lymphoma. *PLoS One* **6**(2): e16408, 2011.
60) Miyachi M, Tsuchiya K, Yoshida H, *et al*: Circulating muscle-specific microRNA, miR-206, as a potential diagnostic marker for rhabdomyosarcoma. *Biochem Biophys Res Commun* **400**(1): 89-93, 2010.
61) 宮地　充，土屋邦彦，浅井大介・他: 筋特異的microRNAは横紋筋肉腫の新規血清腫瘍マーカーである. 日整会誌 **85**(6): S848, 2011.
62) Valadi H, Ekström K, Bossios A, *et al*: Exosome-mediated transfer of mRNAs and microRNAs is a novel mechanism of genetic exchange between cells. *Nat Cell Biol* **9**(6): 654-659, 2007.
63) 窪田大介，末原義之，藤原智洋・他: microRNAマイクロアレイを用いた骨肉腫化学療法奏効性予測バイオマーカーの開発. 日整会誌　**86**(6): S967, 2012.

9．2'-OME RNAオリゴを基盤とした独特の二次構造をもつ新規microRNA阻害剤S-TuD

原口　健・伊庭英夫

われわれは，これまでに特定のmicroRNA(miRNA)を阻害するdecoy RNA, TuD RNA(tough decoy RNA)をプラスミドベクターやウイルスベクターから発現させる系を開発してきた。このベクターはそれまでのmiRNA阻害RNA発現ベクターと比べて極めて高い阻害能を有していることから，様々なmiRNA解析において用いられてきた。われわれは核酸創薬をめざし，この独特の二次構造をもつTuD RNAの構造を模した2'-OME RNAオリゴを合成し，高い阻害活性をもたせる設計法を確立した。そして，この新規miRNA阻害剤を「S-TuD（synthetic TuD)」と命名した。本稿において，このS-TuDについて紹介したい。

はじめに

本特集で紹介されているようにmicroRNA（miRNA）は様々な生命現象に関わることが明らかにされつつあり，数年前からは基礎研究の対象としてだけではなく治療標的としても注目を集めはじめている。こうした視点から特定のmiRNAを阻害する技術は，研究ツールとしてだけではなく，miRNAを標的とした治療法の基本技術として必須となってきた。これまでにわれわれは特定のmiRNAの配列を認識してその活性を阻害するdecoy RNA（TuD RNA：tough decoy RNA）を設計し，これをRNAポリメラーゼIIIにより高レベル発現させるユニットを搭載したプラスミドベクターやレトロ/レンチウイルスベクターを開発してきた[1]。TuD RNAは特徴的な二次構造を有していて，従来のdecoy RNAに比べて著しく高い阻害効果を発揮することから，miRNAを対象とした基礎研究において有用なツールとしてmiRNAの標的の決定[2]，発がん活性の検定[3]をはじめとした幅広い分野[4)-8)]で使用されている。しかし，TuD RNA発現ウイルスベクターを治療に直接使用するためには遺伝子治療の必要があるが，残念なことにそれにはまだ，わが国では課題が多いのが現状である。そこで今回われわれはこの基盤技術の核酸医薬化をめざして，TuD RNAの二次構造を模した2本の2'-OME RNA[用解]核酸オリゴで構成される分子を合成し，S-TuD（synthetic TuD）と名づけて，その最適の設計法を開発してきた。最近極めて良好な結果を得ることができたので[9]，本稿では，この新規miRNA阻害剤S-TuDの設計法，効果，利用法などを紹介する。

key words
miRNA，miRNA阻害剤，TuD RNA，miR-21，miR-200c，miR-16，seed，miRNAファミリー，ZEB1

Ⅰ．新規miRNA阻害剤S-TuDの設計法

1．S-TuDの基本構造

われわれがすでに確立したTuD RNAの基本構造を図❶Aに示した。1分子のTuD RNAは18bpのステム構造Ⅰ，標的miRNAに相補な配列MBS（miRNA binding site）を2つ，8bpのステム構造Ⅱをもつステムループ，2つのMBSと2つのステム構造それぞれとを連結する3ntのリンカー配列4つから構成されている[1]。これらの構造はそれぞれ，核外輸送，標的miRNAへの結合，RNaseやmiRNA-RISC複合体による分解への耐性，MBSとmiRNAの結合しやすさ（accessibility）の向上に寄与してTuD RNAの優れた標的miRNA阻害活性を支えているものと考えられる。そこでわれわれは，このTuD RNAの独特の二次構造を模したオリゴヌクレオチドを合成することとした（S-TuD, synthetic TuD）。TuD RNAは120nt程度の長さの1本のRNAであるが，この長さのRNAを高効率で安価に合成することは困難である。そのため図❶Bに示すように，S-TuDは60nt弱の長さの2本のRNA鎖をアニールすることにより作製し，RNaseに対する耐性を高めるためにすべてのリボースを2'-OMe化することにした。

2．MBS配列の検討

miRNAとMBSの親和性は，もちろん完全相補である場合に最も高くなることが期待される。しかし，TuD RNAはMBS配列として標的のmiRNAに完全相補な配列の3'端から10番目と11番目の間に4nt挿入した配列（バルジ）をもっている。この塩基間でRISC複合体中のAgo2が標的mRNAを切断することが知られており[10]，この4nt挿入によりTuD RNAはRISC複合体による切断を回避することができる。一方，S-TuDは2'-OME RNAオリゴで構成されているのでRISC複合体による切断も受けにくいものと考えられる。そこでまずmiR-21を標的としたS-TuDのMBS配列について，標的miRNAに完全相補な配列である"pf"，標的miRNAの5'端から10番目の塩基に対してのみミスマッチを導入した"10mut"，従来の4ntのバルジを挿入した配列"4ntin"の3種類について検討した。miR-21と完全相補配列を3'-UTRにもつレポーターを使用したアッセイでは，miR-21活性の阻害効果はS-TuD-miR21-10mut，S-TuD-miR21-4ntin，S-TuD-miR21-pfの順に高かった（図❷A）。一方，miR-200cを標的としたS-TuDを用いて同様の検討をしたところ，阻害効果の高さはS-TuD-miR200c-pf，S-TuD-miR200c-10mut，S-TuD-miR200c-4ntinの

図❶　TuD RNAおよびS-TuDの構造（文献9より）

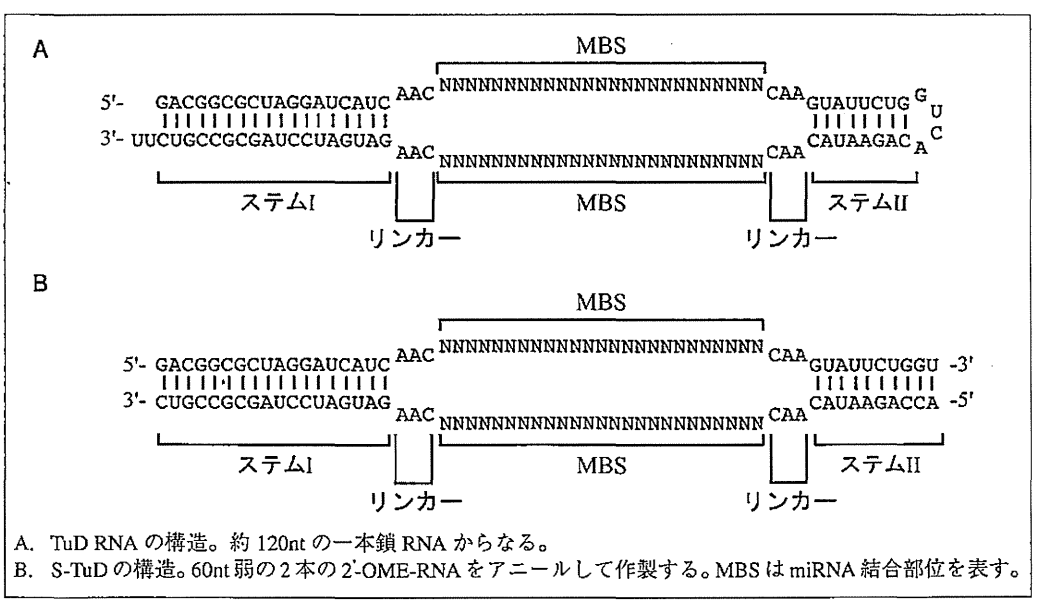

A．TuD RNAの構造。約120ntの一本鎖RNAからなる。
B．S-TuDの構造。60nt弱の2本の2'-OME-RNAをアニールして作製する。MBSはmiRNA結合部位を表す。

図❷ MBS 配列の検討（文献９より）

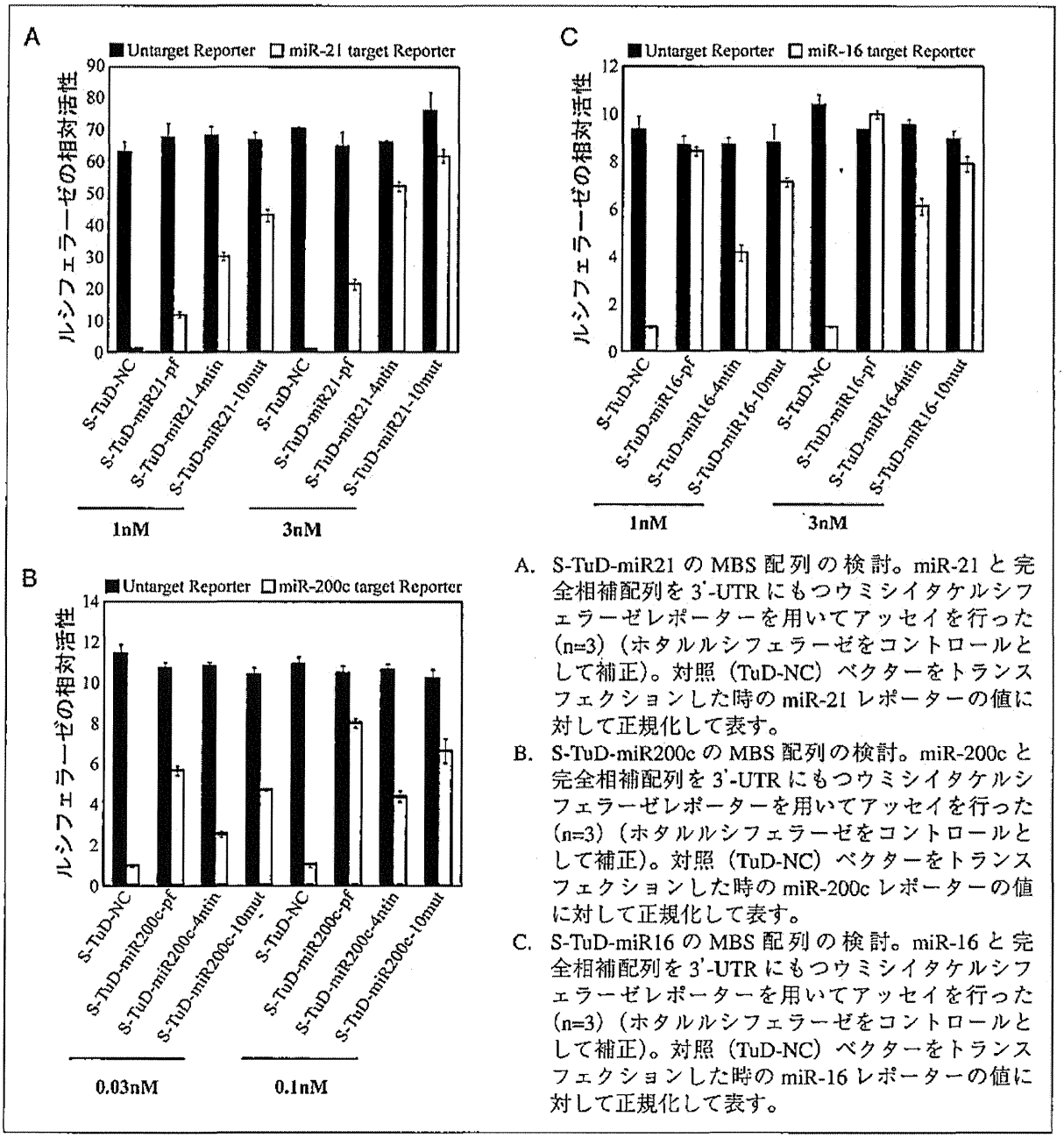

A. S-TuD-miR21 の MBS 配列の検討。miR-21 と完全相補配列を 3'-UTR にもつウミシイタケルシフェラーゼレポーターを用いてアッセイを行った（n=3）（ホタルルシフェラーゼをコントロールとして補正）。対照（TuD-NC）ベクターをトランスフェクションした時の miR-21 レポーターの値に対して正規化して表す。

B. S-TuD-miR200c の MBS 配列の検討。miR-200c と完全相補配列を 3'-UTR にもつウミシイタケルシフェラーゼレポーターを用いてアッセイを行った（n=3）（ホタルルシフェラーゼをコントロールとして補正）。対照（TuD-NC）ベクターをトランスフェクションした時の miR-200c レポーターの値に対して正規化して表す。

C. S-TuD-miR16 の MBS 配列の検討。miR-16 と完全相補配列を 3'-UTR にもつウミシイタケルシフェラーゼレポーターを用いてアッセイを行った（n=3）（ホタルルシフェラーゼをコントロールとして補正）。対照（TuD-NC）ベクターをトランスフェクションした時の miR-16 レポーターの値に対して正規化して表す。

順であった（図❷B）。さらに miR-16 を標的として上述の 3 種類の S-TuD-miR16 を作製して検討を行った（図❷C）。阻害効果は S-TuD-miR16-pf, S-TuD-miR16-10mut, S-TuD-miR16-4ntin の順に高かった。

標的 miRNA ごとに最適な MBS 配列が異なっていたことについて，われわれは S-TuD の二次構造に原因があるのではないかと考えて，これらの S-TuD の二次構造を CentroidFold により予測した[11]。CentroidFold は 2 本の 2'-OME RNA オリゴで構成されている S-TuD には対応していないため，ここでは同じ MBS 配列をもつ TuD RNA の二次構造を代替として予測した。その結果，9 種類の S-TuD のうち，S-TuD-miR21-pf, S-TuD-miR200c-4ntin において MBS 同士が強く結合することがわかった。

このような結果から一般に，より標的 miRNA との結合親和性が高い MBS 配列のほうがより効果的であるが，S-TuD 分子内での MBS 間の結合が強い場合は S-TuD は効果が大きく減弱するものと

図❸　S-TuDのmiRNA阻害効果の濃度依存性および既存技術との比較（文献9より）

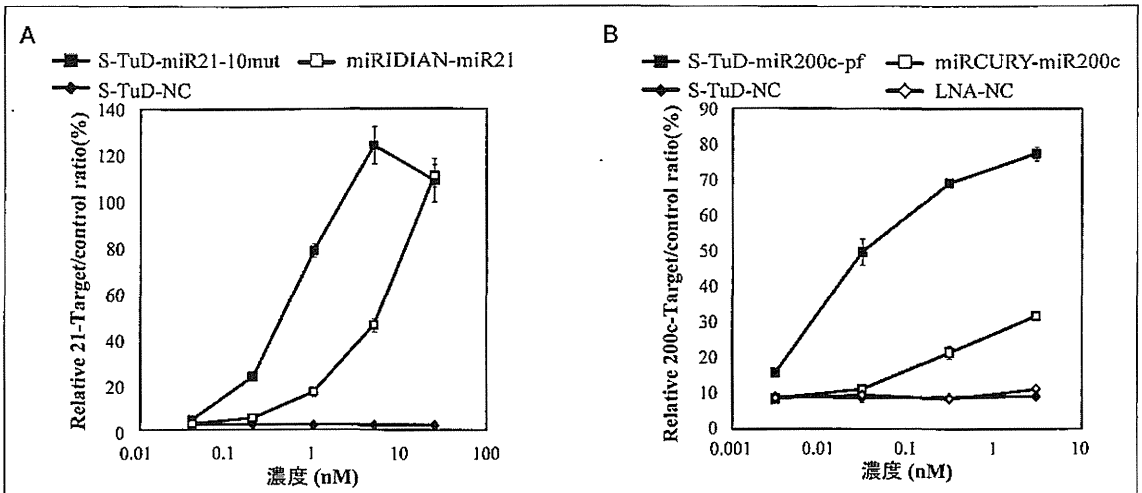

A. S-TuD-miR21-10mutの濃度依存性。0.04nM-0.2nM-1nM-5nM-25nMの範囲でmiRIDIAN-miR21と比較検討した。miR-21と完全相補配列を3'-UTRにもつウミシイタケルシフェラーゼレポーターを用いてアッセイを行った（n=3）（ホタルルシフェラーゼをコントロールとして補正）。miR-21との相補配列を3'-UTRにもたないウミシイタケルシフェラーゼレポーターの値に対する百分率比で表す。

B. S-TuD-miR200c-pfの濃度依存性。0.003nM-0.03nM-0.3nM-3nMの範囲でmiRCURY-miR200cと比較検討した。miR-200cと完全相補配列を3'-UTRにもつウミシイタケルシフェラーゼレポーターを用いてアッセイを行った（n=3）（ホタルルシフェラーゼをコントロールとして補正）。miR-200cとの相補配列を3'-UTRにもたないウミシイタケルシフェラーゼレポーターの値に対する百分率比で表す。

考えられる。そこで，われわれはMBS配列設計法として，まず親和性の視点から"pf"，"10mut"，"4ntin"の順に候補とし，二次構造予測においてMBS間結合が強い場合は順次，次の候補を選択する方法をとっている。

Ⅱ．S-TuDのmiRNA阻害活性

1．S-TuDのmiRNA阻害活性の濃度依存性と既存の阻害剤との比較

S-TuDのmiRNA阻害活性の濃度依存性はどのようなものであろうか。まずmiR-21を標的として，最適と判定されたS-TuD-miR21-10mutについて検討した。さらに既存のmiRNA阻害剤のうち，2'-OME RNAオリゴで構成されるmiRIDIAN（Thermo Scientific社）との比較を行った（図❸A）。S-TuD-miR21-10mutは0.2nMで阻害効果がみられはじめ，5nMで阻害効果が飽和点に達していた。一方，miRIDIAN-miR21は1nMで阻害効果がみられはじめ，25nMで阻害効果が飽和点に達した。次にmiR-200cを標的として，S-TuD-miR200c-pfについて検討した。そして既存のmiRNA阻害剤のうち，DNAとLNA[用語2]のキメラオリゴで構成されるmiRCURY（Exiqon社）との比較を行った（図❸B）。S-TuD-miR200c-pfは0.003nMで阻害効果がみられはじめ，0.3nMで阻害効果が飽和点に達した。一方，miRCURY-miR200cは3nMにおいても阻害効果が飽和点に達しなかった。以上の結果は，S-TuDは既存技術と比べ極めて低い濃度で高い阻害効果を発揮することを示している。S-TuDの有効な濃度は標的miRNAごとに異なることがわかったが，これは主として標的miRNAの発現量が多ければより投与量が要求されることを反映しているものと考えられる。

2．標的miRNAのファミリー間における特異性

特異性を評価するために，標的miRNAと同一のseed配列（5'端から2-8番目の塩基）をもつmiRNAファミリーに対してS-TuDがどの程度miRNA阻害能を有するかについて検討した。標的miRNAファミリーとしてまずmiR-200c/-429を選択し，S-TuD-miR200c-pfとS-TuD-miR429-pfのmiR-200c

図❹ miRNA ファミリーに対する S-TuD の阻害効果（文献９より）

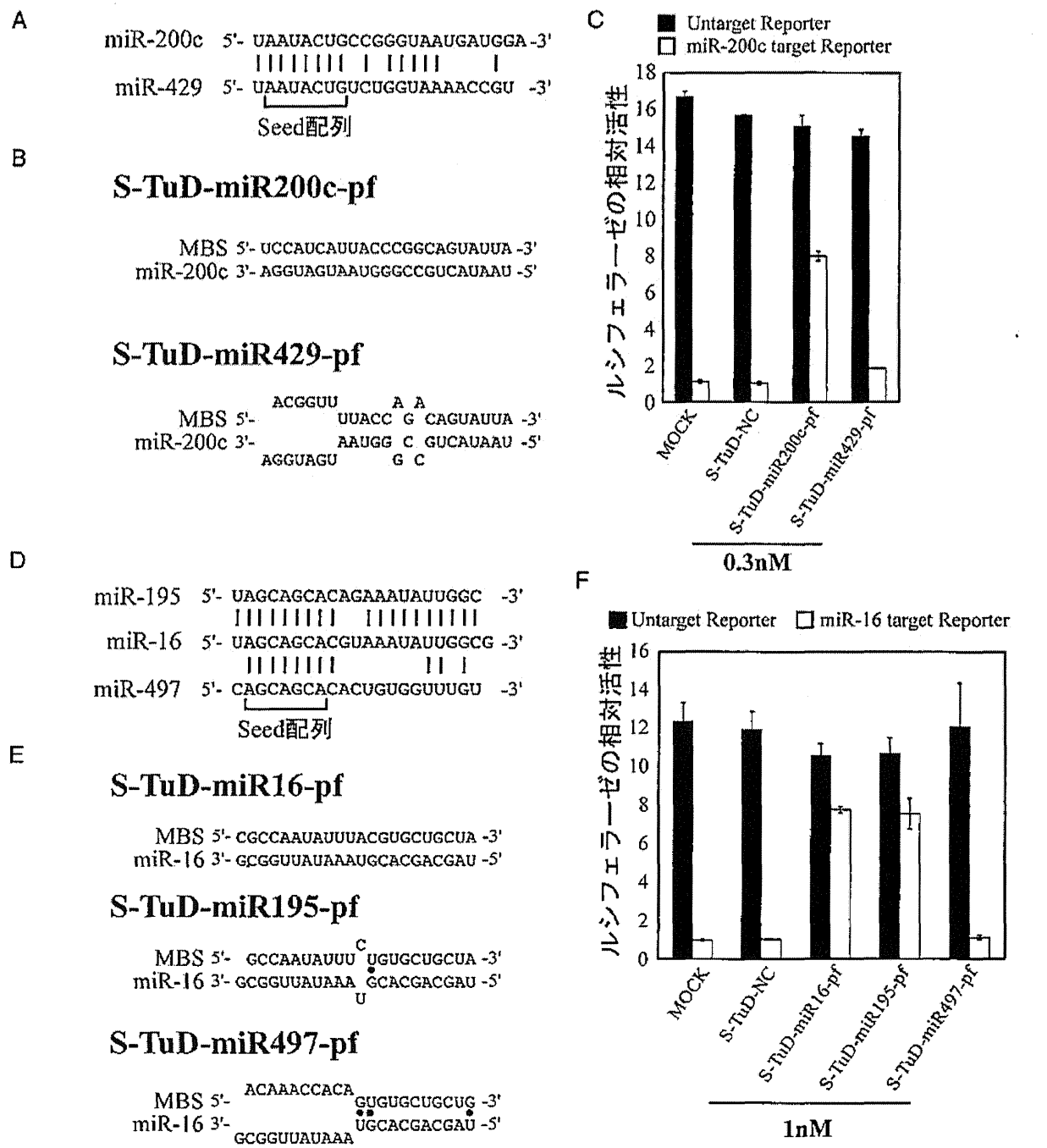

A. miR-200c, miR-429 間の相同性を示す。
B. S-TuD-miR200c-pf, S-TuD-miR429-pf それぞれの MBS と miR-200c の結合様式を示す。
C. miR-200c と完全相補配列を 3'-UTR にもつウミシイタケルシフェラーゼレポーターを用いてアッセイを行った (n=3)（ホタルルシフェラーゼをコントロールとして補正)。対照（TuD-NC）ベクターをトランスフェクションした時の miR-200c レポーターの値に対して正規化して表す。
D. miR-16, miR-195, miR-497 間の相同性を示す。
E. S-TuD-miR16-pf, S-TuD-miR195-pf, S-TuD-miR497-pf それぞれの MBS と miR-16 の結合様式を示す。ドットは G-U ペアを示す。
F. miR-16 と完全相補配列を 3'-UTR にもつウミシイタケルシフェラーゼレポーターを用いてアッセイを行った (n=3)（ホタルルシフェラーゼをコントロールとして補正)。対照（TuD-NC）ベクターをトランスフェクションした時の miR-16 レポーターの値に対して正規化して表す。

に対する阻害能を測定した（図❹A, B, C）。アッセイにはHCT-116細胞を用いたが，この細胞内ではmiR-200cの発現量が高くmiR-429の発現量は低いため，このアッセイではmiR-429の影響をほとんど受けないものと考えられる。S-TuD-miR200c-pfはmiR-200cを阻害したが，S-TuD-miR429-pfはmiR-200cを阻害しなかった。次に標的miRNAファミリーとしてmiR-16/-195/-497を選択し，S-TuD-miR16-pf，S-TuD-miR195-pf，S-TuD-miR497-pfのmiR-16に対する阻害能を測定した（図❹D, E, F）。HCT-116細胞はmiR-16の発現量が高くmiR-195/-497の発現量は低いため，このアッセイではmiR-195/-497の影響をほとんど受けないものと考えられる。S-TuD-miR16-pf，S-TuD-miR195-pfはmiR-16を阻害したが，S-TuD-miR497-pfはmiR-16を阻害しなかった。以上のことから，S-TuDの標的認識にはseed配列だけでは不十分であって，miRNAの3'側に対しても高い相補性が必要であり，S-TuDが高い標的特異性を有することが示された。

3. miRNA阻害能の持続性

S-TuDのmiRNA阻害能の持続性について検討した。S-TuDがトランスフェクションされた細胞とされなかった細胞を区別するために，S-TuDを構成する2本の2'-OME RNAオリゴのうち，片方の5'端に5-FAM修飾を施した5-FAM-S-TuD（5-FAM-S-TuD-NC，5-FAM-S-TuD-miR200c-pf）を作製した。そしてHCT-116細胞にトランスフェクションして2日後に5-FAM陽性細胞をFACSにて分取して培養を続けた。そしてトランスフェクションから2，7，11日後にmiR-200cルシフェラーゼレポーターを用いてアッセイを行ったところ（図❺A），7日後までは高い阻害効果を維持していた。実際に，この時期の細胞では，miR-200cの標的の1つであるZEB1の発現が上昇している（図❺B）。この結果から，細胞分裂を繰り返す細胞においても7日程度阻害効果が持続することがわかった。本アッセイに用いたHCT-116細胞は倍加時間が16～18時間であり，S-TuD-miR200c-pfの導入によって増殖がやや落ちるものの，細胞分裂速度の速い細胞である[12]。そのため本アッセイにおいては細胞分裂によってS-TuDはかなり希釈されてしまっているにもかかわらず7日程度阻害効果が持続したこと

図❺　S-TuDのmiRNA阻害効果の持続性（文献9より）

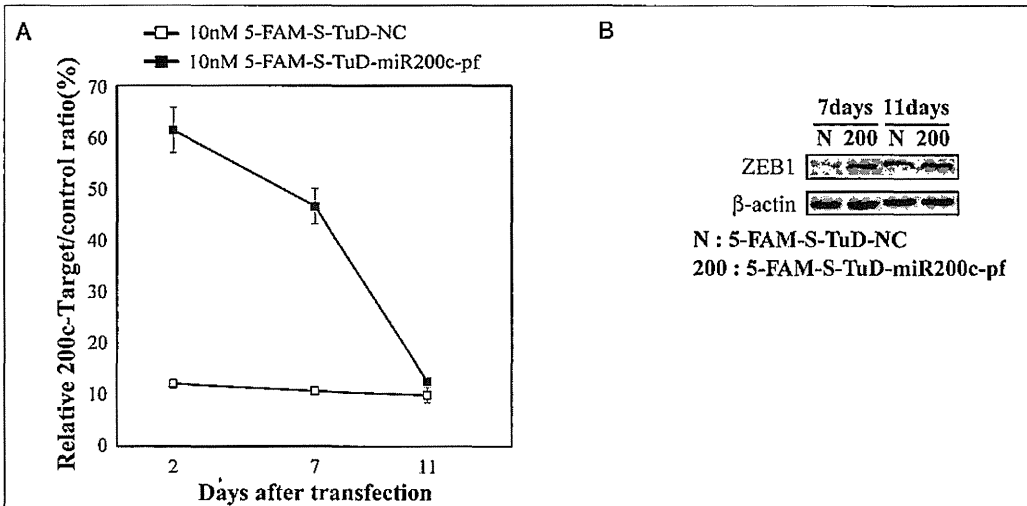

A. S-TuD-miR200c-pfの持続性。5-FAM標識したS-TuD-miR200c-pfとS-TuD-NCをHCT-116細胞へトランスフェクションして2日後に図❸Bと同様のレポーターアッセイを行った。さらにこれと同時に一部の細胞からFACS sortingにより5-FAM陽性細胞を分取した。これらの細胞の培養を続け，トランスフェクションから7，11日後に図❸Bと同様のレポーターアッセイを行った。

B. さらに，これらの分取細胞におけるmiR-200c標的遺伝子であるZEB1の発現量をウェスタンブロットにより測定した。β-アクチンをローディングコントロールとして用いた。

から，分裂速度の遅い細胞またはほとんど分裂しない細胞においてはS-TuDの効果はさらに長い期間持続するのではないかと考えられる。

おわりに

本稿で紹介したように，S-TuDは既存のmiRNA阻害剤と比較しても高い阻害能を有している。miRNA阻害ベクターであるTuD RNAと目的に応じて使い分けることにより，効率よくmiRNAの機能解析を進めることができると考えられる。また本特集で紹介されているように，特定のmiRNAが，がん・炎症免疫・感染症などの幅広いヒト疾患において，創薬標的として地位をかためつつある。今後われわれはS-TuDをmiRNAを標的とした治療薬として確立していきたい。このようなRNA創薬を実現化するためには，*in vivo*におけるS-TuDの動態や効果，副作用の有無などの解析を進めるとともに，適切なドラッグデリバリーシステムを探索することが今後の課題である。

用語解説

1. 2'-OME RNA：リボース骨格の2位にあるOH基がメチル化修飾されたRNAを指す。非修飾RNAと比べ，RNAとの結合親和性やヌクレアーゼ耐性が高い。
2. LNA：リボース骨格の2位の酸素原子と4位の炭素原子が架橋された核酸類縁体 locked nucleic acidを指す。非修飾RNAと比べ，RNAとの結合親和性やヌクレアーゼ耐性が高い。

参考文献

1) Haraguchi T, Ozaki Y, et al：Nucleic Acids Res 37, e43, 2009.
2) Sakurai K, Furukawa C, et al：Cancer Res 71, 1680-1689, 2011.
3) Lu Z, Li Y, et al：EMBO J 30, 57-67, 2011.
4) Hikichi M, Kidokoro M, et al：Mol Ther 19, 1107-1115, 2011.
5) Gagan J, Dey BK, et al：J Biol Chem 286, 19431-19438, 2011.
6) Matsuyama H, Suzuki H, et al：Blood 118, 6881-6892, 2011.
7) Xie Q, Chen X, et al：Cancer 118, 2431-2442, 2012.
8) Sakurai F, Furukawa N, et al：Virus Res 165, 214-218, 2012.
9) Haraguchi T, Nakano H, et al：Nucleic Acids Res 40, e58, 2012.
10) Elbashir SM, Lendeckel W, et al：Genes Dev 15, 188-200, 2001.
11) Sato K, Hamada M, et al：Nucleic Acids Res 37, W277-W280, 2009.
12) 秋山　徹，河府和義：細胞・培地活用ハンドブック，26-27, 羊土社，2008.

参考ホームページ

- miRBase
  http://www.mirbase.org/
- ncRNA-CentroidFold
  http://www.ncrna.org/centroidfold

原口　健

2004年　東京大学理学部生物化学科卒業
2006年　同大学院理学系研究科生物化学専攻修士課程修了
　　日本学術振興会特別研究員（DC1）
2009年　東京大学大学院理学系研究科生物化学専攻博士課程修了（理学博士）
　　東京大学医科学研究所感染免疫部門宿主寄生体学分野助教

これまでmicroRNA阻害ベクターの開発や，今回紹介したmicroRNA阻害剤の開発を行ってきました。現在はこれらの技術を用いてがんにおけるmicroRNAの機能解明を行うとともに，これらの技術の改良・応用を進めています。

THE JOURNAL OF BIOLOGICAL CHEMISTRY VOL. 287, NO. 15, pp. 11924–11933, April 6, 2012

Double Plant Homeodomain (PHD) Finger Proteins DPF3a and -3b Are Required as Transcriptional Co-activators in SWI/SNF Complex-dependent Activation of NF-κB RelA/p50 Heterodimer*[S]

Received for publication, November 10, 2011, and in revised form, January 30, 2012 Published, JBC Papers in Press, February 13, 2012, DOI 10.1074/jbc.M111.322792

Aya Ishizaka[‡1], Taketoshi Mizutani[‡§], Kazuyoshi Kobayashi[‡], Toshio Tando[‡], Kouhei Sakurai[‡], Toshinobu Fujiwara[¶], and Hideo Iba[‡2]

From the [‡]Division of Host-Parasite Interaction, Department of Microbiology and Immunology, Institute of Medical Science, University of Tokyo, 4-6-1 Shirokanedai, Minato-ku, Tokyo 108-8639, [§]RNA and Biofunctions, PRESTO, Japan Science and Technology Agency, 4-1-8 Honcho, Kawaguchi, Saitama 332-0012, and the [¶]Institute of Microbial Chemistry Laboratory of Disease Biology, 3-14-23 Kamiosaki, Shinagawa-ku, Tokyo 141-0021, Japan

Background: The NF-κB dimer, RelA/p50, often requires the SWI/SNF complex for its transactivation function, but its molecular mechanisms remain elusive.
Results: The NF-κB canonical pathway induced by TNF-α is DPF3a/b- and SWI/SNF-dependent for some promoters.
Conclusion: DPF3a and DPF3b are effective linkers for the SWI/SNF complex and RelA/p50.
Significance: The NF-κB·DPF3a/b·SWI/SNF complex would be an effective platform for promoter-specific transactivation.

We have previously shown that DPF2 (requiem/REQ) functions as a linker protein between the SWI/SNF complex and RelB/p52 NF-κB heterodimer and plays important roles in NF-κB transactivation via its noncanonical pathway. Using sensitive 293FT reporter cell clones that had integrated a SWI/SNF-dependent NF-κB reporter gene, we find in this study that the overexpression of DPF1, DPF2, DPF3a, DPF3b, and PHF10 significantly potentiates the transactivating activity of typical NF-κB dimers. Knockdown analysis using 293FT reporter cells that endogenously express these five proteins at low levels clearly showed that DPF3a and DPF3b, which are produced from the *DPF3* gene by alternative splicing, are the most critical for the RelA/p50 NF-κB heterodimer transactivation induced by TNF-α stimulation. Our data further show that this transactivation requires the SWI/SNF complex. DPF3a and DPF3b are additionally shown to interact directly with RelA, p50, and several subunits of the SWI/SNF complex *in vitro* and to be co-immunoprecipitated with RelA/p50 and the SWI/SNF complex from the nuclear fractions of cells treated with TNF-α. In ChIP experiments, we further found that endogenous DPF3a/b and the SWI/SNF complex are continuously present on HIV-1 LTR, whereas the kinetics of RelA/p50 recruitment after TNF-α treatment correlate well with the viral transcriptional activation levels. Additionally, re-ChIP experiments showed DPF3a/b and the SWI/SNF complex associate with RelA on the endogenous *IL-6* promoter after TNF-α treatment. In conclusion, our present data indicate that by linking RelA/p50 to the SWI/SNF complex, DPF3a/b induces the transactivation of NF-κB target gene promoters in relatively inactive chromatin contexts.

NF-κB[3] is a key transcription factor that regulates many biological processes, such as immune, inflammatory, and virus responses, development, cellular growth, and apoptosis. The regulation by NF-κB is achieved through the transactivation of a large number of its target genes in a cell type-specific and/or stimulus-specific manner (1–4). NF-κB is itself composed of homo- or heterodimeric complexes of members of the NF-κB family of proteins, which include RelA (p65), RelB, c-Rel, p50, and p52 in humans. NF-κB dimers remain inactive in the cytoplasm until specific stimulation activates their signaling pathways (5). One of the main NF-κB pathways, the canonical pathway, is triggered by stimulation with factors such as tumor necrosis factor-α (TNF-α) and lipopolysaccharide (LPS). The induction of this pathway results in the activation of the RelA/p50 heterodimer by transporting it to the nucleus after phosphorylation and also the proteasomal degradation of inhibitor of NF-κB (IκB), which retains RelA/p50 in the cytoplasm under unstimulated conditions (6). However, RelB/p52, which is present in the cytoplasm as inactive RelB/p100 (NF-κB1) until stimulated, is activated through the noncanonical pathway (7). This pathway is triggered by stimuli such as lymphotoxin exposure, and it induces the cleavage of cytosolic p100 to produce p52, which subsequently translocates into the nucleus as a RelB/p52 dimer.

* This work was supported by Grants-in-aid for Scientific Research on Priority Areas 17016015 and for Scientific Research (B) 22300318 and (C) 21590507 from the Ministry of Education, Culture, Sports, Science and Technology, Japan, and by a grant from the Japan Society for the Promotion of Science.
[S] This article contains supplemental Figs. S1-S9, Table S1, and experimental procedures.
[1] Research Fellow of the Japan Society for the Promotion of Science.
[2] To whom correspondence should be addressed: Division of Host-Parasite Interaction, Dept. of Microbiology and Immunology, Institute of Medical Science, University of Tokyo, 4-6-1 Shirokanedai, Minato-ku, Tokyo 108-8639, Japan. Tel.: 81-3-5449-5730; Fax: 81-3-5449-5449; E-mail: iba@ims.u-tokyo.ac.jp.

[3] The abbreviations used are: NF-κB, nuclear factor-κB; PHD, plant homeodomain; Luc, luciferase.

The mechanism by which each NF-κB dimer is recruited to a certain set of promoters and specifically transactivates their transcription in a cell type-dependent manner is an important question. Such processes would likely involve chromatin context-dependent regulation. Indeed, NF-κB transactivation is known to often require the SWI/SNF complex, a representative chromatin remodeling factor involved in epigenetic regulation in humans, but no clear and direct interaction between NF-κB components and the SWI/SNF complex has been reported. The SWI/SNF complex has two alternative ATPases, Brahma (Brm) or Brahma-related gene 1 (BRG1) as the catalytic subunits, and other subunits such as BAF155, Ini1/SNF5, BAF170, BAF60a, and β-actin (8–10). The SWI/SNF complex is recruited to target genes via association with transcription regulators such as c-Myc (11), C/EBPβ (12), AP-1 (13), neuron-restrictive silencer factor (14), and Cdx2 (15). In addition to cellular targets, we have shown that integrated LTRs of murine leukemia virus (16, 17) and HIV-1 (human immunodeficiency virus-1) (18) require the Brm-type SWI/SNF complex to maintain their gene expression.

We have recently shown that DPF2 (REQ/BAF45d) functions as an efficient adaptor protein between the SWI/SNF complex and RelB/p52 and plays important roles in NF-κB transcriptional activation at the most downstream part of the NF-κB noncanonical pathway (19). DPF2 belongs to the d4 family of proteins, the members of which are characterized by an N-terminal 2/3 domain containing a nuclear localization signal, a central C2H2-type Krüppel-like zinc finger motif, and a C-terminal d4 domain consisting of a tandem repeat of the PHD zinc finger (20–22). It was previously shown that another member of the d4 family, DPF3 (Cerd4/BAF45c), associates with the SWI/SNF complex and further that the *DPF3* gene has two splicing variants, the products of which differ at their C-terminal regions. The DPF3b protein shows all of the characteristics of a d4 family member, including binding activity to either methylated or acetylated lysine residues at histones H3 and H4 through the PHD fingers. However, DPF3a lacks these binding activities as it harbors a truncated d4 domain within its first PHD (23). Interestingly, two d4 family members, DPF1 (Neud4/BAF45b) and DPF3, and an additional protein, PHF10 (BAF45a), which also possesses double PHD fingers within its C terminus, have been reported to associate with the SWI/SNF complex in neural cells in a differentiation-specific manner (24). In mouse neural progenitors, the complex contains PHF10, but this component is substituted by DPF1 or DPF3 when the cells become differentiated into post-mitotic neurons.

Considering our previous finding that DPF2 is required for RelB/p52 transactivation via the SWI/SNF complex, we speculate that the five proteins DPF1, DPF2, DPF3a, DPF3b, and PHF10 are candidate co-activators of the typical NF-κB heterodimer, RelA/p50, as well as two other NF-κB dimers, RelB/p52 and c-Rel/p50. We show in our current analysis that each of these proteins can enhance the different NF-κB heterodimers to transactivate their targets efficiently when both they and the NF-κB components are exogenously expressed. We further show from our analysis that among these five proteins DPF3a and DPF3b are the most effective cofactors for RelA/p50 activation in 293FT cells treated with TNF-α. Our current data further indicate that these two proteins directly bind to RelA, p50, and at least four subunits of the SWI/SNF complex *in vitro*. We additionally show that endogenous DPF3a/b and the SWI/SNF complex are continuously co-localized at the HIV-1 LTR throughout the period of TNF-α stimulation and that RelA/p50 is promptly recruited to the typical NF-κB-binding sites within the HIV-1 LTR or endogenous *IL-6* promoter upon stimulation. Finally, we show that the viral transcripts are synthesized with similar kinetics to those of RelA/p50 recruitment.

EXPERIMENTAL PROCEDURES

Cell Culture and Retro- and Lentiviral Vectors—293FT cells (Invitrogen) were maintained in Dulbecco's modified Eagle's medium (Wako Chemicals, Tokyo) containing 10% fetal calf serum at 37 °C and 5% CO_2. For TNF-α stimulation, the cells were treated with 10 ng/ml TNF-α (R&D Systems, Minneapolis, MN). Vesicular stomatitis virus G protein (VSV-G)-pseudotyped retro- or lentiviral vectors were prepared as described previously (17, 19). For transduction, cells were incubated with the virus vector stocks in the presence of 8 μg/ml Sequabrene™ (Sigma).

Antibodies—Rabbit polyclonal antibodies against human DPF3 were raised against a synthetic peptide corresponding to amino acid residues 230–251 of the protein (NP_036206) by Medical and Biological Laboratories (MBL, Nagoya, Japan). Other antibodies used in this research are as follows: normal rabbit IgG (PM035) (MBL), α-RelA (C-20), α-BRG-1 (H-88), α-BAF155 (H-76) (Santa Cruz Biotechnology, Santa Cruz, CA), α-p105/p50 (ab7971), α-Brm (ab15597) (Abcam, Cambridge, MA), α-FLAG (M2) (Sigma), α-BAF60a (611728), and α-Ini1 (612110) (BD Transduction Laboratories, San Jose, CA). Most of these specific antibodies are rabbit polyclonal, except α-FLAG, α-BAF60a, and α-Ini1 which are mouse monoclonal.

GST Fusion Protein Pulldown Assays—GST fusion proteins were expressed in *Escherichia coli* Rosetta 2 (Novagen, Madison, WI) via incubation of the cells with 0.1 mM isopropyl 1-thio-β-D-galactopyranoside overnight at 15 °C and then prepared using His tag Binding/Wash Buffer (20 mM Tris-HCl (pH 8.0), 600 mM NaCl, 1 mM $MgCl_2$, 10% glycerol, 0.1% Nonidet P-40, 20 mM imidazole, and phosphatase inhibitors). Purification of GST-His-tagged proteins was performed sequentially using Profinity IMAC nickel-charged resin (Bio-Rad) and glutathione-Sepharose 4B (GE Healthcare). The target proteins were eluted from these columns with His tag Elution Buffer (20 mM Tris-HCl (pH 8.0), 600 mM NaCl, 1 mM $MgCl_2$, 10% glycerol, 0.1% Nonidet P-40, 250 mM imidazole, and phosphatase inhibitors) and GST Elution Buffer (100 mM Tris-HCl (pH 8.0), 12 mM NaCl, 20 mM glutathione, and phosphatase inhibitors), respectively. *In vitro* transcription and translation were then performed as described previously (19). *In vitro* synthesized proteins were incubated with respective GST fusion proteins for 2 h at 4 °C on a rotating platform. The complexes were washed for five times with TNE buffer (10 mM Tris-HCl (pH 7.8), 150 mM NaCl, 1 mM EDTA, 1% Nonidet P-40, and protease inhibitors) and analyzed by SDS-PAGE followed by autoradiography using FLA-5100 (Fujifilm). Cellular lysates, prepared in TN buffer (10 mM Tris-HCl (pH 7.8), 150 mM NaCl, 1% Nonidet P-40, protease inhibitors, and phosphatase inhibitors) were

treated with 100 units/ml benzonase endonuclease (Novagen) and precleared by incubation with GST protein immobilized on beads for 1 h. The lysate was then incubated with respective GST fusion proteins for 4 h at 4 °C on a rotating platform. The complexes were subsequently washed three times with Buffer D (20 mM HEPES-KOH (pH 7.9), 20% glycerol, 0.1 M KCl, 0.2 mM EDTA, 0.1% Nonidet P-40, and protease inhibitors) and analyzed by immunoblotting.

Chromatin Immunoprecipitation (ChIP) and Sequential ChIP Assays—Cells were cross-linked with 1% formaldehyde at 37 °C for 8 min. Cross-linking reactions were stopped by the addition of a 0.1 volume of 1.5 M glycine and incubation at room temperature for 5 min. The cells were then washed with PBS, collected, and incubated in lysis buffer 1 (50 mM HEPES (pH 7.5), 140 mM NaCl, 1 mM EDTA, 10% glycerol, 0.5% Nonidet P-40, 0.25% Triton X-100, and protease inhibitors). Cell lysates were sequentially replaced with lysis buffer 2 (10 mM Tris-HCl (pH 8.0), 200 mM NaCl, 1 mM EDTA, 0.5 mM EGTA, and protease inhibitors), and lysis buffer 3 (10 mM Tris-HCl (pH 8.0), 300 mM NaCl, 1 mM EDTA, 0.5 mM EGTA, 0.1% sodium deoxycholate, 0.5% *N*-lauroylsarcosine, and protease inhibitors). The lysates were then sonicated using Elestein Ryuseikai (Elekon Science. Corp., Chiba, Japan) on ice so that the DNA would be sheared into small fragments with an average length of less than 0.5 kb. After the addition of a 0.1 volume of 10% Triton X-100, the lysates were centrifuged to remove cellular debris and incubated overnight on a rotating platform at 4 °C with the respective antibodies (10 μg of each), which were previously bound to Dynabeads protein G (Invitrogen). The beads were washed once in low salt buffer (20 mM Tris-HCl (pH 8.0), 150 mM NaCl, 2 mM EDTA, 0.1% SDS, 1% Triton X-100, and protease inhibitors), twice in high salt buffer (20 mM Tris-HCl (pH 8.0), 400 mM NaCl, 2 mM EDTA, 0.1% SDS, 1% Triton X-100, and protease inhibitors), five times in RIPA buffer (50 mM HEPES (pH 7.6), 500 mM LiCl, 1 mM EDTA, 0.1% SDS, 1% Triton X-100, and protease inhibitors), and once in a TE, 50 mM NaCl buffer. The immune complexes were harvested in elution buffer (10 mM Tris-HCl (pH 7.5), 1 mM EDTA, 1% SDS and 100 mM DTT). For re-ChIP assays, the eluted complexes were diluted 1:10 with dilution buffer (10 mM Tris-HCl (pH 7.5), 150 mM NaCl, 1 mM EDTA, 0.5% sodium deoxycholate, 1% Nonidet P-40, and protease inhibitors), and the steps of ChIP assay were repeated. Cross-linking was reversed by incubation overnight at 65 °C with a 0.04 volume of 5 M NaCl. After treatment with proteinase K (Wako), the DNA was purified using Nucleospin Extract II (Macherey-Nagel, Düren, Germany) and quantified by real time PCR on a 7300 Real Time PCR System (Applied Biosystems, Bedford, MA) using Premix Ex Taq (Probe qPCR) or SYBR Premix Ex Taq (Takara Bio, Shiga, Japan). The specific primer pairs and probes used in this study are listed in supplemental Table S1.

Other Procedures—Details of the materials and methods used in this study can be found in the supplemental experimental procedures.

RESULTS

High Expression of Each Member of the d4 Family and PHF10 Enhances the Transactivating Activity of RelA/p50, RelB/p52, and c-Rel/p50—We previously generated a 293FT cell line stably harboring an exogenous expression unit composed of tandem NF-κB-responsive elements, a minimum promoter (MinP), and the downstream luciferase (Luc) reporter gene (293FT-NF-κB-MinP-Luc) (Fig. 1*A*) (Ref 19), in which the NF-κB-binding sites were derived from HIV-1 LTR (Fig. 1*B*). Whereas this reporter cell system was useful in evaluating chromosome structure-dependent NF-κB transactivation, it was found not to be as sensitive in responding to the exogenous introduction of NF-κB. We thus isolated several additional cellular clones from this parental reporter cell population and tested each for Luc inducibility following TNF-α treatment. A clone, which we designated as 293FT-NF-κB-MinP-Luc-A3, (abbreviated as NF-κB-MinP-Luc-A3 hereafter), showed one of the highest levels of Luc inducibility by TNF-α and was selected for further analysis (supplemental Fig. S1).

Expression vectors for the five co-activator candidate proteins, four d4 family proteins and PHF10 (supplemental Fig. S2), as well as the empty vector (CV-1) as a control were transfected into NF-κB-MinP-Luc-A3 together with each pair of plasmids expressing the NF-κB dimer, RelA/p50, RelB/p52, or c-Rel/p50, as well as the control vector for NF-κB expression (CV-2). The expression of these five candidate proteins that were tagged with FLAG at their N termini were confirmed by immunoblotting (supplemental Fig. S3*A*). As shown in Fig. 1*C*, the basal Luc activity in cells transfected with CV-2 was not significantly affected by the introduction of any of the candidate proteins (*lanes 2–6* compared with *lane 1*). Compared with the Luc activity of cells transfected with CV-1, the introduction of RelA/p50, RelB/p52, and c-Rel/p50 increased these reporter expression levels by 42-, 6-, and 3-fold, respectively (Fig. 1*C*, *lanes 13, 19,* and *7* compared with *lane 1*). These results indicated that NF-κB-MinP-Luc-A3 has very low basal NF-κB activity and that none of the candidates have any effects alone under these conditions, even if expressed at high levels. Importantly, transactivation mediated through RelA/p50 (Fig. 1*C*, *lanes 14–18* compared with *lane 13*), RelB/p52 (*lanes 20–24* compared with *lane 19*), and c-Rel/p50 (*lanes 8–12* compared with *lane 7*) was enhanced by the endogenous expression of any of the five candidate proteins (*lanes 7–24*). No significant differences were found among these five proteins in terms of the enhancement of any of the three NF-κB dimers, suggesting that all potentially function as co-activators of NF-κB in any context, at least when expressed at high levels.

Both DPF3a and DPF3b Are Required for SWI/SNF-dependent Transcriptional Activation through the NF-κB Canonical Pathway—We concluded that transfection experiments involving NF-κB expression vectors would not fully reflect NF-κB activation induced by naturally occurring signal transduction pathways and that the transient expression of candidate proteins by plasmid vectors is very high and thus far from physiological (supplemental Fig. S4). Hence, the experimental conditions used above would most likely not reflect the functional specificity of these proteins correctly. We thus examined the requirement for each candidate protein in the activation of NF-κB by TNF-α treatment, which strongly and almost exclusively activates the endogenous RelA/p50 dimer. Because 293FT cells express all of the transcripts coding these five can-

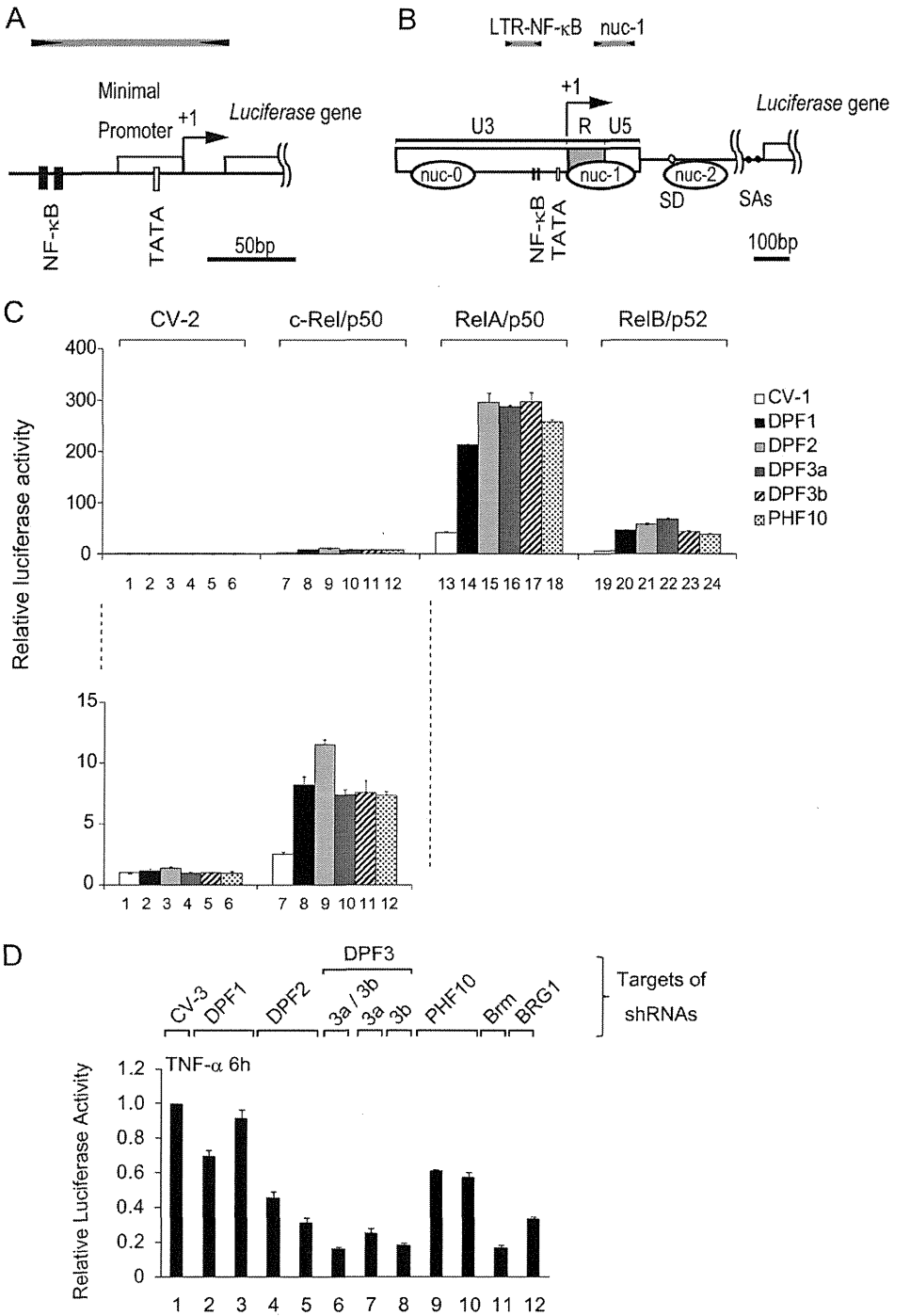

FIGURE 1. **d4 family members are potentially involved in both the canonical and noncanonical NF-κB transactivation of SWI/SNF-dependent promoters.** *A* and *B*, schematic representation of the constructs used in this study: NF-κB-MinP (*A*) and HIV-1 LTR (*B*). The binding sites for NF-κB and the TATA boxes are highlighted by *black* and *white bars*, respectively. Transcriptional start sites are designated as +1. Positions detected by real time PCR are indicated by *black arrows* and *gray bars*. The splicing donor and the acceptors are indicated by *white* and *black circles*. *C*, NF-κB-MinP-Luc-A3 cells were cotransfected with 10 ng of vectors expressing NF-κB subunits and 490 ng of candidate protein expressing or respective control vectors in different combinations. Luciferase activity was measured 48 h after transfection and normalization using control plasmid transfectants. *D*, NF-κB-MinP-Luc-A3 cells were transfected with 500 ng of vectors expressing short hairpin RNAs against each candidate protein and also *Brm* or *BRG1*. At 42 h post-transfection, cells were treated with 10 ng/ml TNF-α for 6 h, which led to a 1500-fold activation of luciferase activity compared with the control vector (CV-3) transfectants (data not shown). Luciferase activities were normalized to the CV-3 control transfectants. The corresponding target sites of the shRNAs against each of the candidates analyzed in this experiment are shown in supplemental Fig. S1. *Lane 2*, shDPF1-cds-1; *lane 3*, shDPF1-utr-1; *lane 4*, shREQ#1; *lane 5*, shREQ#2; *lane 6*, shDPF3-cds-1; *lane 7*, shDPF3a-utr-2; *lane 8*, shDPF3b-cds-3; *lane 9*, shPHF10-cds-1; and *lane 10*, shPHF10-utr-1. The results presented here are the average of at least three independent experiments, and the *bars* indicate the standard deviation.

didate proteins, as judged by semi-quantitative RT-PCR (supplemental Fig. S3*B* and data not shown), we performed knockdown experiments using the same assay cell line, NF-κB-MinP-Luc-A3. The efficiency and specificity of each of the designed shRNAs were confirmed by semi-quantitative RT-PCR or immunoblotting using 293FT cells (supplemental Fig. S3, *B* and

C). The NF-κB-MinP-Luc-A3 cell line was transfected with a vector that expresses shRNA targeting each candidate protein and the catalytic subunits of the SWI/SNF complex as well as a control shRNA vector (CV-3). At 42 h after transfection, cultures were treated with or without TNF-α for an additional 6 h.

Upon TNF-α stimulation, Luc activity increased by 1400-fold when the cells were transfected with CV-3. The knockdown of Brm and BRG1, the alternative catalytic subunits of the SWI/SNF complex, caused a significant reduction in transactivation by 82 and 66%, respectively (Fig. 1*D*, *lanes 11* and *12*), indicating that NF-κB-MinP in the reporter cell line requires the SWI/SNF complex to be activated through the NF-κB canonical pathway. The depletion of DPF2 (Fig. 1*D*, *lanes 4* and *5*) and PHF-10 (Fig. 1*D*, *lanes 9* and *10*) lowered the ability of TNF-α to activate this promoter by 60 and 40% respectively, and the knockdown of DPF1 (Fig. 1*D*, *lanes 2* and *3*) marginally but clearly reduced the Luc promoter activity. These results are consistent with the notion deriving from the results of the overexpression experiments (Fig. 1*C*) that DPF1, DPF2, and PHF10 contribute to transactivation via the endogenous RelA/p50 dimer and the difference among the effects of each knockdown might be somehow reflecting their endogenous levels. Interestingly, the simultaneous depletion of DPF3a and DPF3b by a single shRNA, whose targeting site is within the shared region for these proteins, was shown to reduce TNF-α-dependent activation by 84% (Fig. 1*D*, *lane 6*). Furthermore, a single knockdown of either DPF3a or DPF3b also caused a comparative reduction in promoter activation (Fig. 1*D*, *lanes 7* and *8*). These results suggest that in these cells, among the tested candidates, either DPF3a or DPF3b have the most crucial role in the canonical NF-κB pathway, which cannot be efficiently compensated for by the other candidate proteins. The overall results shown in Fig. 1*D* were almost identically obtained using another 293FT clone K5 (supplemental Fig. S5). Taken together, these data support the idea that in 293FT cells DPF3a and DPF3b are the most critical factors required for RelA/p50 to activate this NF-κB-containing promoters in an SWI/SNF-dependent manner, and we therefore decided to further concentrate our analysis on DPF3a and DPF3b.

Both DPF3a and DPF3b Directly Bind to RelA and p50 as Well as Several Subunits of the SWI/SNF Complex in Vitro—Because DPF3a and DPF3b were found to be required for SWI/SNF complex-dependent RelA/p50 transactivation, we next evaluated the proteins with which DPF3a and DPF3b can associate *in vitro*. We first performed glutathione *S*-transferase pulldown assays using purified GST alone, GST-DPF3a, and -DPF3b and several subunits of the SWI/SNF complex translated *in vitro* in the presence of [^{35}S]methionine (supplemental Fig. S6). Both DPF3a and DPF3b directly bound to Brm, BRG1, Ini1, and BAF60a but not to β-actin, which are similar binding properties to those of DPF2 that we have previously reported (19).

We next performed a similar assay using *in vitro* translated RelA and p50 and GST-fused DPF3a and DPF3b as well as DPF2. As shown in Fig. 2*A*, either RelA or p50 alone as well as in combination with both proteins synthesized in the same translating mixture were found to directly associate with DPF3a and DPF3b. We also found that RelA or p50 alone also binds to DPF2 to a lesser extent. These binding properties of DPF2 are fully consistent with our previous report (19). In the current experiments, these two GST proteins were tagged with His_6 at their C termini to enable higher purification and the performance of a more sensitive binding assay (supplemental Fig. S7). We performed further GST pulldown assays using the same purified GST proteins and 293FT whole cell extracts obtained from cells stimulated with or without TNF-α as the input proteins. The extracts were treated with benzonase endonuclease to avoid detecting interactions mediated through DNA or RNA fragments. The pulled down cellular proteins were analyzed by immunoblotting, and as shown in Fig. 2*B*, both DPF3a and DPF3b were found to associate with endogenous RelA and BRG1. Importantly, the binding affinities for DPF3a and DPF3b in these cases were not significantly increased by TNF-α stimulation. It should be pointed out here that in the total protein preparations subcellular localization of natural NF-κB is disrupted. These results therefore suggest that the binding potential of RelA to DPF3a and DPF3b is not significantly enhanced by post-translational modifications of RelA triggered by TNF-α stimulation (25–28). Taken together, our findings indicate that both DPF3a and DPF3b have the potential to directly associate with RelA/p50 and the SWI/SNF complex and further that the binding potential is not enhanced by post-translational modifications of NF-κB or the SWI/SNF complex triggered by TNF-α.

DPF3 Interacts with the SWI/SNF Complexes and RelA/p50 in the Nucleus—We prepared 293FT cells stably expressing either FLAG-tagged DPF3a or DPF3b through the introduction of retrovirus vectors (293FT-FLAG-DPF3a and 293FT-FLAG-DPF3b) and isolated nuclear fractions from each cell type with or without TNF-α treatment. We then performed a co-immunoprecipitation assay using α-FLAG antibodies (Fig. 2*C*). The subunits of the SWI/SNF complex, Brm, BRG1, and BAF155, were found to be co-immunoprecipitated with either DPF3a or DPF3b, independently of TNF-α stimulation. In the immunoprecipitates with FLAG-DPF3b, both RelA and p50 were detected specifically in TNF-α-stimulated cells, indicating that DPF3b efficiently associates with both RelA and p50, which are recruited to the nucleus. In the immunoprecipitates with FLAG-DPF3a from TNF-α-stimulated cells, p50 was detected, whereas only marginal levels of RelA were detectable, suggesting that DPF3a binds RelA/p50 at a lower affinity than DPF3b in the nucleus. Our observations therefore suggest that the association between DPF3a/b and RelA/p50 occurs following RelA/p50 translocation to the nucleus where DPF3a or -3b consistently interacts with the SWI/SNF complex. When similar analyses were performed on the other candidate proteins, DPF1 and DPF2 showed similar binding properties to DPF3a and -3b for the associations with the SWI/SNF complex and RelA/p50 (supplemental Fig. S8).

To further analyze the DPF3 interaction with the RelA/p50 and SWI/SNF complex, we prepared whole cell extracts from 293FT-FLAG-DPF3a and 293FT-FLAG-DPF3b with or without TNF-α treatment (Fig. 2*D*). Each cellular extract was again treated with benzonase endonuclease and then subjected to a co-immunoprecipitation assay using α-FLAG antibodies. Brm, BRG1, BAF155, and BAF60a were all successfully co-immunoprecipitated from the total cellular lysates of both 293FT-

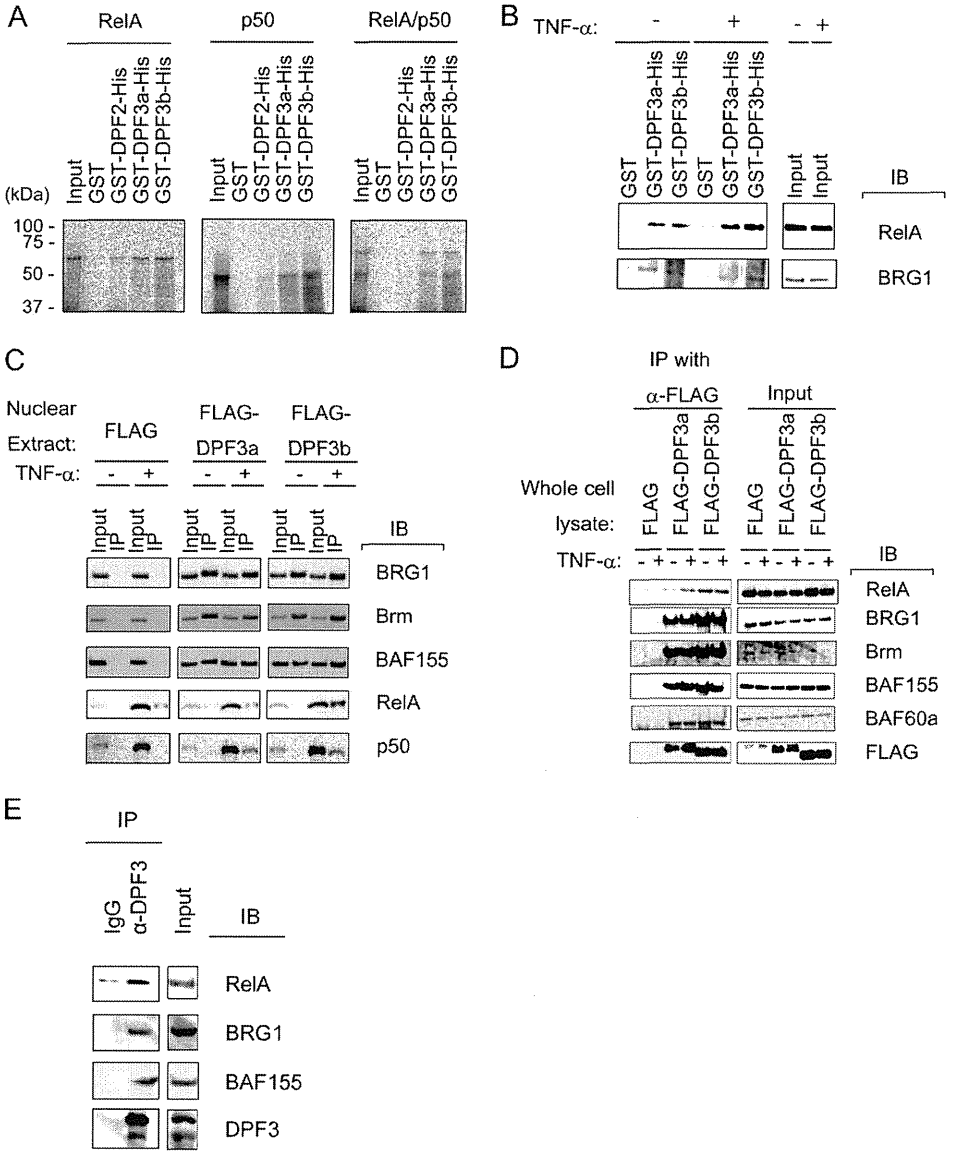

FIGURE 2. **DPF3a and -3b associate with both RelA/p50 and the SWI/SNF complex.** *A*, [^{35}S]methionine-labeled RelA and p50 were translated using a wheat germ extract system *in vitro* and incubated with GST alone and GST-His-tagged DPF2, DPF3a, or DPF3b. These interactions were analyzed by SDS-PAGE followed by autoradiography. *B*, 293FT cells were stimulated with or without 10 ng/ml TNF-α for 10 min, and whole cell lysates were then obtained and subjected to benzonase endonuclease treatment. The lysate was incubated with GST alone, GST-His-tagged DPF2, DPF3a, or DPF3b, and pulled down materials were analyzed by immunoblotting. *C*, 293FT cells were stimulated with or without 10 ng/ml TNF-α for 10 min, and whole cell lysates were obtained and treated with endonuclease. Immunoprecipitation (*IP*) assays were performed using α-FLAG antibodies, and precipitated materials were eluted with free FLAG peptide and analyzed by immunoblotting (*IB*). *D*, 293FT cells stably expressing FLAG, FLAG-DPF3a, or FLAG-DPF3b were stimulated with or without 10 ng/ml TNF-α for 60 min. Nuclear extracts were then prepared and subjected to immunoprecipitation assays with α-FLAG antibodies followed by immunoblotting. *E*, 293FT cells were treated with 10 ng/ml TNF-α for 20 min, and whole cell lysate was obtained and treated with endonuclease. Immunoprecipitation assays were performed using α-DPF3 antibody, and precipitated materials were analyzed by immunoblotting.

FLAG-DPF3a and -DPF3b independently of TNF-α. RelA was found to be co-immunoprecipitated with DPF3b and to a lesser extent with DPF3a. DPF3a and DPF3b would associate with RelA after the preparation of the whole cell extracts from unstimulated cells, where the natural NF-κB subcellular localizations are disrupted. These data again support that the RelA binding potential to DPF3a or DPF3b was not significantly affected by TNF-α treatment, consistent with the results shown in Fig. 2*B*.

To finally show our observations that DPF3a/b associates with RelA/p50 or the SWI/SNF complex is valid even in non-manipulated cells, we treated 293FT cells with TNF-α for 20 min and immunoprecipitated endogenous DPF3a and DPF3b with antibody against DPF3, which does not discriminate between DPF3a and DPF3b. The immunoprecipitates were analyzed, and endogenous DPF3a/b was shown to associate with RelA, BRG1, and BAF155, just like exogenously introduced DPF3 proteins (Fig. 2*E*).

Kinetics of RelA Recruitment upon TNF-α Stimulation Correlate with Those of Primary Transcript Production from Both Artificial and Natural Promoters—To understand molecular mechanisms involved in transcriptional activation after TNF-α stimulation, we next analyzed the kinetics of RelA recruitment and transactivation. Following cellular exposure to TNF-α, it

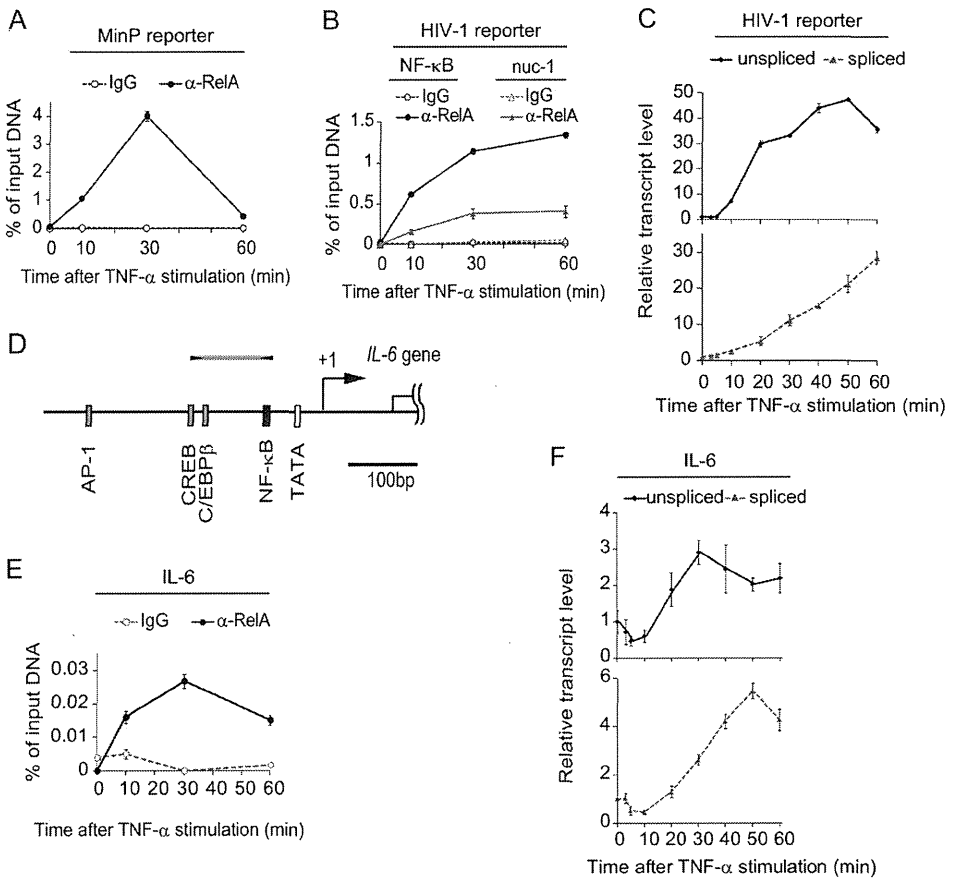

FIGURE 3. **Kinetics of RelA recruitment upon TNF-α stimulation correlate with the primary transcript production levels from both artificial and native promoters.** *A, B,* and *E,* kinetics of RelA recruitment to NF-κB-MinP (*A*), HIV-1 LTR (*B*), and the endogenous IL-6 promoter (*E*) upon TNF-α stimulation. Cells were treated with 10 ng/ml TNF-α for the indicated times and were harvested and precipitated by antibodies against RelA or with a normal rabbit IgG control. The immunoprecipitated DNA was quantified by real time PCR and normalized relative to the input. *C* and *F*, real time RT-PCR analysis of transcripts of HIV-1 LTR (*C*) and the endogenous IL-6 promoter (*F*). Cells were treated with 10 ng/ml TNF-α for the indicated times, and mRNA was prepared. Spliced and unspliced mRNAs were quantified, and these levels were normalized to individual untreated samples. *D*, schematic representation of the *IL-6* promoter region. The binding site for NF-κB and other transcription factors and the TATA box are highlighted by *black, gray,* and *white bars*, respectively. Transcriptional start sites are designated as +1. Positions detected by real time PCR are indicated by *black arrows* and a *gray bar.*

was previously reported at a single cell resolution that RelA oscillates dynamically between the nucleus and the cytoplasm and that this oscillation cycle is about 1 h (29). To analyze the primary effects of TNF-α stimulation on RelA/p50 transactivation, we performed ChIP analysis of the promoters of the reporter genes after stimulation within 1 h. In NF-κB-MinP-Luc-A3 cells, the results showed that the stimulation-dependent recruitment of RelA achieved a peak at 30 min post-treatment and drastically reduced to marginal levels within 60 min (Fig. 3*A*). Next, by using 293FT cells harboring an HIV-1-based reporter provirus (293FT-LTR-Luc-5; Fig. 1*B*) instead, we performed the same set of analyses (Fig. 3*B*). Interestingly, RelA recruitment to the NF-κB-responsive elements within the HIV-1 LTR kept increasing during the first 60 min after TNF-α stimulation with small leakage of the signal detected in the nucleosome 1 (nuc-1) region. Considering that the nucleotide sequences of the NF-κB elements are identical in both of these promoters, it is noteworthy that distinct kinetics of RelA recruitment were observed, *i.e.* the wild type HIV-1 LTR retains RelA longer.

We next analyzed whether there was any association between the recruitment levels of RelA and the transactivation kinetics of these promoters. By quantifying the HIV-1 LTR transcript levels at the indicated time points by real time RT-PCR, we found that the kinetics of the *de novo* synthesized primary unspliced mRNAs were very similar to those of RelA recruitment, whereas those of the mature spliced mRNAs kept increasing (Fig. 3*C*). Because the primary transcript of NF-κB-MinP does not contain introns, it cannot be distinguished from the mature mRNA. Interestingly, using a promoter of an endogenous TNF-α-inducible gene, IL-6 (Fig. 3*D*), which requires the SWI/SNF complex for activation (14), we observed a good correlation in kinetics between RelA recruitment and primary transcript synthesis after TNF-α stimulation (Fig. 3, *E* and *F*, and the induction kinetics is more prompt than those observed for HIV-1 LTR in the same cells (Fig. 3*B*). In addition, the kinetics of the recruitment of RelA to the *IL-6* promoter are similar to those of NF-κB-MinP, achieving a peak at 30 min after stimulation and decreasing at 60 min. Our present observations thus suggest that HIV-1 LTR retains RelA longer against the oscillation cycle of RelA between the nucleus and the cytoplasm. HIV-1 LTR contains many binding sites for other transcription factors, some of which would associate with RelA (30–32). This might cause differences in the kinetics of the

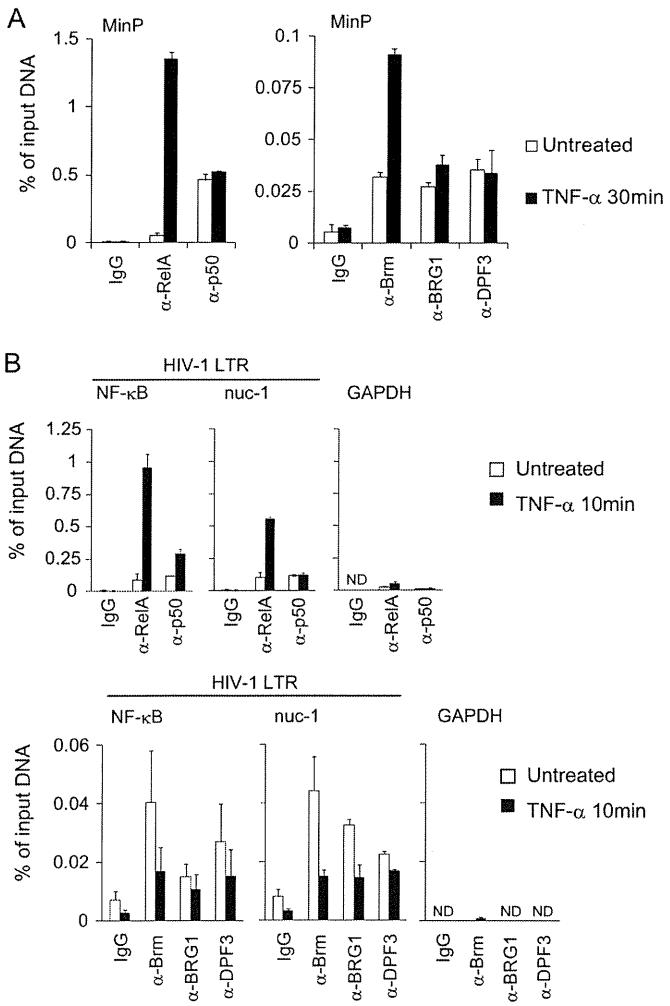

FIGURE 4. **Chromatin dynamics and recruitment of DPF3 and RelA/p50 to SWI/SNF-dependent promoters upon TNF-α treatment.** ChIP analysis was performed, and the data were quantified as described in Fig. 3. *A*, ChIP analysis of RelA, p50, Brm, BRG1, and DPF3 levels at the NF-κB-MinP upon TNF-α stimulation. *B*, recruitment of RelA, p50, Brm, BRG1, BAF60a, Ini1, and DPF3 to the regions within the HIV-1 LTR and GAPDH promoter after TNF-α treatment. Results presented here are the average of at least two independent experiments. *ND*, not detectable.

artificial MinP, which is simply under the control of NF-κB. However, the endogenous *IL-6* promoter is also regulated by other transcription regulators but showed no retention of RelA. This observation might be reflecting that, unlike HIV-1 LTR, this gene is expected to be strictly down-regulated after the stimulation for proper inflammatory response.

Chromatin Dynamics around the NF-κB-binding Sites in Both Artificial and Native Promoters after TNF-α Treatment—We next analyzed the dynamics of endogenous DPF3 and the SWI/SNF complex as well as RelA/p50 for both NF-κB-MinP and HIV-1 LTR in response to TNF-α stimuli. Consistent with Fig. 3*A*, this stimulation caused a dynamic recruitment of RelA to NF-κB-MinP at 30 min (*left panel* of Fig. 4*A*). Similar amounts of NF-κB p50 subunit were detected both before and after TNF-α stimulation, which we think is consistent with previous observations that low levels of the p50 subunit are present on specific NF-κB-responsive promoters in the nucleus of unstimulated cells as the p50 homodimer, whereas the majority of this subunit is retained in the cytoplasm as RelA/p50 (33–35). The p50 homodimer itself does not contain transactivation domains, but it associates with promoter regions of some NF-κB-dependent genes, including integrated HIV-1 LTR in the unstimulated conditions (36). However, Brm, BRG1, and DPF3 were all detected at the promoter even before stimulation, and their recruitment levels were not significantly changed upon exposure to TNF-α, apart from Brm, which showed elevated levels at the promoter (*right panel* of Fig. 4*A*). In the case of 293FT-LTR-Luc-5 cells, RelA was recruited to NF-κB elements in the HIV-1 LTR within 10 min of stimulation, whereas the NF-κB p50 subunit was found to be constitutively present in the LTR (*upper panel* of Fig. 4*B*). Brm, BRG1, and DPF3 were also detected at the promoter prior to TNF-α treatment, and their recruitment levels were reduced by about 50% after stimulation, suggesting that upon transcriptional activation, the SWI/SNF complex partially releases from the promoter with DPF3 (*lower panel* of Fig. 4*B*). Because other subunits of the complex such as BAF60a and Ini1 behaved in a similar manner to Brm or BRG1 (supplemental Fig. S9), we speculate that the changes in the levels of the catalytic subunits associated with the HIV-LTR promoter were as part of the SWI/SNF complex.

Whereas the two promoters under analysis showed different RelA recruitment kinetics, they were found to share two important features from our observations. First, endogenous DPF3 together with the SWI/SNF complex is bound to the promoters prior to TNF-α stimulation. Second, upon stimulation, RelA/p50, which can directly interact with DPF3 (Fig. 2*A*), was found to be rapidly recruited to the promoters, and this recruitment was shown to be associated with transcriptional activation, as judged by the primary transcript levels.

Finally, we analyzed the endogenous *IL-6* promoter to check whether DPF3 links the SWI/SNF complex and RelA/p50 forming a larger complex. ChIP analysis showed that both RelA and DPF3a/b were recruited to the promoter in a TNF-α-dependent and -independent manner, respectively (Fig. 5*A*). To perform sequential ChIP analysis, the immunoprecipitates with α-RelA antibody were re-immunoprecipitated with antibodies specific for DPF3a/b and Brm as well as the α-RelA antibody (positive control) and normal rabbit IgG (negative control), respectively (Fig. 5*B*). The second round of immunoprecipitates using α-DPF3 and Brm antibodies indicated that DPF3 and the SWI/SNF complex co-associate with RelA on the *IL-6* promoter after the RelA/p50 heterodimer is recruited upon TNF-α stimulation. In conclusion, all these results support that DPF3a and -3b link the SWI/SNF complex to NF-κB to transactivate the target promoters that require chromatin remodeling for the transcriptional initiation.

DISCUSSION

By extending our previous observation that DPF2 links RelB/p52 and the SWI/SNF complex for NF-κB transactivation via its noncanonical pathway, we have here shown that each of the five proteins, DPF1, DPF2, DPF3a, DPF3b, and PHF10, can equally function as an efficient co-activator of the RelA/p50 dimer at the most downstream part of the NF-κB canonical pathway, when they are exogenously expressed at high levels

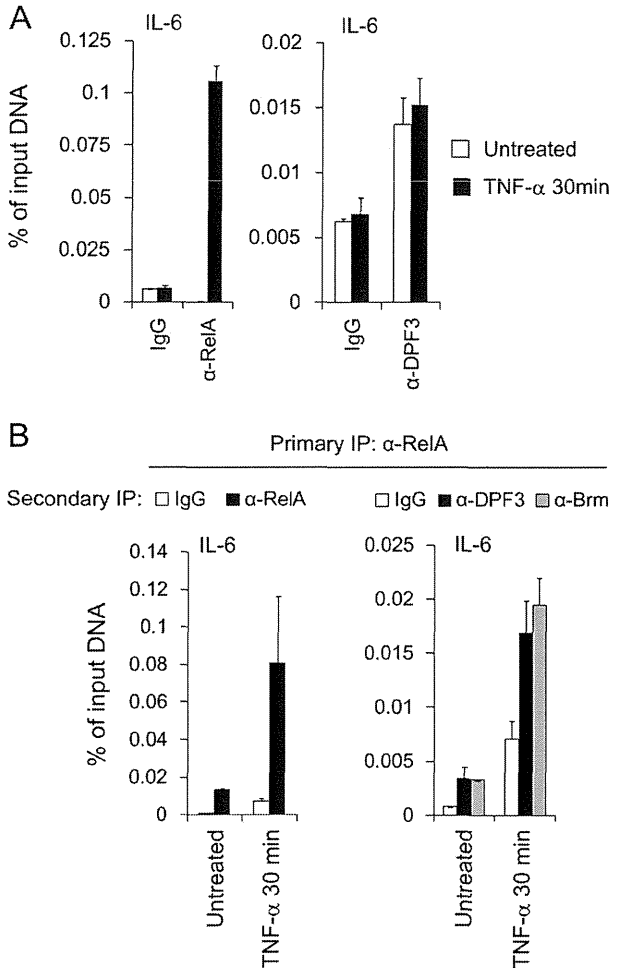

FIGURE 5. **ChIP and re-ChIP assays at the endogenous *IL-6* promoter.** *A*, ChIP analysis of RelA and DPF3 occupancy levels at the *IL-6* promoter. 293FT cells were treated with or without 10 ng/ml TNF-α for 30 min and harvested for precipitation by antibodies against RelA and DPF3. *B*, primary immunoprecipitated materials concentrated with α-RelA antibody were followed by secondary rounds of immunoprecipitations with indicated antibodies. Immunoprecipitated materials were quantified by real time PCR.

(Fig. 1*C*). Under these conditions, each of these proteins activated the other two representative NF-κB dimers, RelB/p52 and c-Rel/p50, with similar efficiencies. When these five proteins were expressed by retrovirus vectors, they are constitutively binding to the SWI/SNF complex in the nucleus and begin to associate with RelA/p50 upon TNF-α treatment (Fig. 2*C* and supplemental Fig. S8). From these results, we think each of these proteins would function as a co-activator of NF-κB in certain tissues. DPF1 was reported to be neurospecific and play an important role in developing neurons (20, 24). DPF2, which is ubiquitously expressed, is known to be involved in the processes of apoptosis in mouse myeloid cells following interleukin 3 (IL-3) deprivation (37). In normal cells, DPF3a/b was reported to be expressed specifically in cardiac and skeletal muscle and was critical for heart and muscle development (23). Because NF-κB plays important roles in programmed cell death and development, these d4 proteins might be involved in these physiological phenomena through activating some specific NF-κB dimers. Because DPF1, DPF2, DPF3b and PHF10 contain double PHD fingers, which are not possessed by any of the core subunits of the SWI/SNF complex, they are likely to play some roles in selecting specific species of modified histones in the nucleosomes at target promoter regions.

In 293FT cells, which express only low levels of endogenous mRNAs for the five candidate protein co-activators, the knockdown of either DPF3a or DPF3b suppressed TNF-α-induced NF-κB transactivation to marginal levels, suggesting that both proteins are essential for the NF-κB canonical pathway (Fig. 1*D*). Currently, we cannot fully explain this observation, but there could be several possibilities. One possibility would be that the SWI/SNF complex needs to bind both DPF3a and DPF3b to perform its full function for NF-κB transactivation. We would, however, prefer another possibility as follows. DPF3a and DPF3b share roles in NF-κB transactivation probably through their common N-terminal regions. The endogenous cellular amounts of both proteins in 293FT cells are so low (supplemental Fig. S3) that depletion of either would drastically reduce their recruitment frequency to the promoter of the reporter, where a single molecule of either DPF3a or DPF3b is sufficient for the SWI/SNF complex to perform full transactivation. Because DPF3a lacks functional PHD fingers, however, it is also possible that they would show distinct promoter preferences in some cases, as has been shown previously by ChIP analysis of exogenously expressed DPF3a and DPF3b (23).

We have previously shown that a representative target gene of the NF-κB canonical pathway, *IL-8*, is induced in HeLa cells by TNF-α and that this induction is not affected by the knockdown of DPF2. We suggested from this that DPF2 does not significantly contribute to the NF-κB canonical pathway, at least in this cell system. Because the endogenous *IL-8* gene was found not to be affected by the knockdown of either catalytic subunit of the SWI/SNF complex (19), we believe that this promoter is induced independently of SWI/SNF. In immune cells, some NF-κB target promoters have also been reported not to require chromatin remodeling for their transcriptional initiation upon LPS stimulation, because they already possess an open chromosome structure (38).

Importantly, with respect to our current investigations, the results of ChIP analysis using antiserum that we prepared indicated that the endogenous DPF3 proteins (this antiserum does not discriminate between DPF3a and DPF3b) as well as the SWI/SNF complex are recruited continuously to the promoters we examined, NF-κB-MinP and wild type HIV-1 LTR. Considering that both DPF3a and DPF3b directly bind to p50 *in vitro*, we speculate that DPF3a/3b together with the SWI/SNF complex locate near the NF-κB-binding sites through the binding of the p50 homodimer under unstimulated conditions but through active RelA/p50 upon stimulation. This dimer substitution would then trigger SWI/SNF-dependent transactivation. Hence, the SWI/SNF complex would be present at these target promoters to facilitate the ready recruitment of RelA/p50 for the prompt remodeling of the surrounding chromatin structures. Considering our observations that transcriptional enhancement of HIV-1 LTR occurs just after the SWI/SNF complex and RelA/p50 get together on the promoter (Figs. 3, *B* and *C*, and 4*B*), DPF3a/3b is significant for this activation as a linker protein.

Acknowledgments—We thank S. Kawaura and A. Kato for their assistance in preparing this manuscript. We thank Dr. H. Nakano and Dr. H. Watanabe for critical reading of this manuscript.

REFERENCES

1. Beinke, S., and Ley, S. C. (2004) Functions of NF-κB1 and NF-κB2 in immune cell biology. *Biochem. J.* **382,** 393–409
2. Santoro, M. G., Rossi, A., and Amici, C. (2003) NF-κB and virus infection. Who controls whom. *EMBO J.* **22,** 2552–2560
3. Vallabhapurapu, S., and Karin, M. (2009) Regulation and function of NF-κB transcription factors in the immune system. *Annu. Rev. Immunol.* **27,** 693–733
4. Ben-Neriah, Y., and Karin, M. (2011) Inflammation meets cancer, with NF-κB as the matchmaker. *Nat. Immunol.* **12,** 715–723
5. Gilmore, T. D. (2006) Introduction to NF-kappaB: players, pathways, perspectives. *Oncogene* **25,** 6680–6684
6. Ghosh, S., May, M. J., and Kopp, E. B. (1998) NF-κB and Rel proteins. Evolutionarily conserved mediators of immune responses. *Annu. Rev. Immunol.* **16,** 225–260
7. Pomerantz, J. L., and Baltimore, D. (2002) Two pathways to NF-κB. *Mol. Cell* **10,** 693–695
8. Muchardt, C., and Yaniv, M. (1999) ATP-dependent chromatin remodeling. SWI/SNF and Co. are on the job. *J. Mol. Biol.* **293,** 187–198
9. Wilson, B. G., and Roberts, C. W. (2011) SWI/SNF nucleosome remodelers and cancer. *Nat. Rev. Cancer* **11,** 481–492
10. Kwon, H., Imbalzano, A. N., Khavari, P. A., Kingston, R. E., and Green, M. R. (1994) Nucleosome disruption and enhancement of activator binding by a human SWI/SNF complex. *Nature* **370,** 477–481
11. Cheng, S. W., Davies, K. P., Yung, E., Beltran, R. J., Yu, J., and Kalpana, G. V. (1999) c-MYC interacts with INI1/hSNF5 and requires the SWI/SNF complex for transactivation function. *Nat. Genet.* **22,** 102–105
12. Kowenz-Leutz, E., and Leutz, A. (1999) A C/EBPβ isoform recruits the SWI/SNF complex to activate myeloid genes. *Mol. Cell* **4,** 735–743
13. Ito, T., Yamauchi, M., Nishina, M., Yamamichi, N., Mizutani, T., Ui, M., Murakami, M., and Iba, H. (2001) Identification of SWI.SNF complex subunit BAF60a as a determinant of the transactivation potential of Fos/Jun dimers. *J. Biol. Chem.* **276,** 2852–2857
14. Watanabe, H., Mizutani, T., Haraguchi, T., Yamamichi, N., Minoguchi, S., Yamamichi-Nishina, M., Mori, N., Kameda, T., Sugiyama, T., and Iba, H. (2006) SWI/SNF complex is essential for NRSF-mediated suppression of neuronal genes in human nonsmall cell lung carcinoma cell lines. *Oncogene* **25,** 470–479
15. Yamamichi, N., Inada, K., Furukawa, C., Sakurai, K., Tando, T., Ishizaka, A., Haraguchi, T., Mizutani, T., Fujishiro, M., Shimomura, R., Oka, M., Ichinose, M., Tsutsumi, Y., Omata, M., and Iba, H. (2009) Cdx2 and the Brm-type SWI/SNF complex cooperatively regulate villin expression in gastrointestinal cells. *Exp. Cell Res.* **315,** 1779–1789
16. Iba, H., Mizutani, T., and Ito, T. (2003) SWI/SNF chromatin remodeling complex and retroviral gene silencing. *Rev. Med. Virol.* **13,** 99–110
17. Mizutani, T., Ito, T., Nishina, M., Yamamichi, N., Watanabe, A., and Iba, H. (2002) Maintenance of integrated proviral gene expression requires Brm, a catalytic subunit of SWI/SNF complex. *J. Biol. Chem.* **277,** 15859–15864
18. Mizutani, T., Ishizaka, A., Tomizawa, M., Okazaki, T., Yamamichi, N., Kawana-Tachikawa, A., Iwamoto, A., and Iba, H. (2009) Loss of the Brm-type SWI/SNF chromatin remodeling complex is a strong barrier to the Tat-independent transcriptional elongation of human immunodeficiency virus type 1 transcripts. *J. Virol.* **83,** 11569–11580
19. Tando, T., Ishizaka, A., Watanabe, H., Ito, T., Iida, S., Haraguchi, T., Mizutani, T., Izumi, T., Isobe, T., Akiyama, T., Inoue, J., and Iba, H. (2010) Requiem protein links RelB/p52 and the Brm-type SWI/SNF complex in a noncanonical NF-κB pathway. *J. Biol. Chem.* **285,** 21951–21960
20. Buchman, V. L., Ninkina, N. N., Bogdanov, Y. D., Bortvin, A. L., Akopian, H. N., Kiselev, S. L., Krylova OYu., Anokhin, K. V., and Georgiev, G. P. (1992) Differential splicing creates a diversity of transcripts from a neuro-specific developmentally regulated gene encoding a protein with new zinc finger motifs. *Nucleic Acids Res.* **20,** 5579–5585
21. Chestkov, A. V., Baka, I. D., Kost, M. V., Georgiev, G. P., and Buchman, V. L. (1996) The d4 gene family in the human genome. *Genomics* **36,** 174–177
22. Ninkina, N. N., Mertsalov, I. B., Kulikova, D. A., Alimova-Kost, M. V., Simonova, O. B., Korochkin, L. I., Kiselev, S. L., and Buchman, V. L. (2001) Cerd4, third member of the d4 gene family. Expression and organization of genomic locus. *Mamm. Genome* **12,** 862–866
23. Lange, M., Kaynak, B., Forster, U. B., Tönjes, M., Fischer, J. J., Grimm, C., Schlesinger, J., Just, S., Dunkel, I., Krueger, T., Mebus, S., Lehrach, H., Lurz, R., Gobom, J., Rottbauer, W., Abdelilah-Seyfried, S., and Sperling, S. (2008) Regulation of muscle development by DPF3, a novel histone acetylation and methylation reader of the BAF chromatin remodeling complex. *Genes Dev.* **22,** 2370–2384
24. Lessard, J., Wu, J. I., Ranish, J. A., Wan, M., Winslow, M. M., Staahl, B. T., Wu, H., Aebersold, R., Graef, I. A., and Crabtree, G. R. (2007) An essential switch in subunit composition of a chromatin remodeling complex during neural development. *Neuron* **55,** 201–215
25. Chaturvedi, M. M., Sung, B., Yadav, V. R., Kannappan, R., and Aggarwal, B. B. (2011) NF-κB addiction and its role in cancer. "One size does not fit all." *Oncogene* **30,** 1615–1630
26. Perkins, N. D. (2006) Post-translational modifications regulating the activity and function of the nuclear factor κB pathway. *Oncogene* **25,** 6717–6730
27. Schmitz, M. L., Mattioli, I., Buss, H., and Kracht, M. (2004) NF-κB. A multifaceted transcription factor regulated at several levels. *ChemBioChem* **5,** 1348–1358
28. Viatour, P., Merville, M. P., Bours, V., and Chariot, A. (2005) Phosphorylation of NF-κB and IκB proteins. Implications in cancer and inflammation. *Trends Biochem. Sci.* **30,** 43–52
29. Nelson, D. E., Ihekwaba, A. E., Elliott, M., Johnson, J. R., Gibney, C. A., Foreman, B. E., Nelson, G., See, V., Horton, C. A., Spiller, D. G., Edwards, S. W., McDowell, H. P., Unitt, J. F., Sullivan, E., Grimley, R., Benson, N., Broomhead, D., Kell, D. B., and White, M. R. (2004) Oscillations in NF-κB signaling control the dynamics of gene expression. *Science* **306,** 704–708
30. Stevens, M., De Clercq, E., and Balzarini, J. (2006) The regulation of HIV-1 transcription. Molecular targets for chemotherapeutic intervention. *Med. Res. Rev.* **26,** 595–625
31. Rohr, O., Marban, C., Aunis, D., and Schaeffer, E. (2003) Regulation of HIV-1 gene transcription. From lymphocytes to microglial cells. *J. Leukocyte Biol.* **74,** 736–749
32. Pereira, L. A., Bentley, K., Peeters, A., Churchill, M. J., and Deacon, N. J. (2000) A compilation of cellular transcription factor interactions with the HIV-1 LTR promoter. *Nucleic Acids Res.* **28,** 663–668
33. Satou, R., Miyata, K., Katsurada, A., Navar, L. G., and Kobori, H. (2010) Tumor necrosis factor-α suppresses angiotensinogen expression through formation of a p50/p50 homodimer in human renal proximal tubular cells. *Am. J. Physiol. Cell Physiol.* **299,** C750–C759
34. Wu, Z. Z., Chow, K. P., Kuo, T. C., Chang, Y. S., and Chao, C. C. (2011) Latent membrane protein 1 of Epstein-Barr virus sensitizes cancer cells to cisplatin by enhancing NF-κB p50 homodimer formation and down-regulating NAPA expression. *Biochem. Pharmacol.* **82,** 1860–1872
35. Zhong, H., May, M. J., Jimi, E., and Ghosh, S. (2002) The phosphorylation status of nuclear NF-κB determines its association with CBP/p300 or HDAC-1. *Mol. Cell* **9,** 625–636
36. Williams, S. A., Chen, L. F., Kwon, H., Ruiz-Jarabo, C. M., Verdin, E., and Greene, W. C. (2006) NF-κB p50 promotes HIV latency through HDAC recruitment and repression of transcriptional initiation. *EMBO J.* **25,** 139–149
37. Gabig, T. G., Mantel, P. L., Rosli, R., and Crean, C. D. (1994) Requiem. A novel zinc finger gene essential for apoptosis in myeloid cells. *J. Biol. Chem.* **269,** 29515–29519
38. Ramirez-Carrozzi, V. R., Braas, D., Bhatt, D. M., Cheng, C. S., Hong, C., Doty, K. R., Black, J. C., Hoffmann, A., Carey, M., and Smale, S. T. (2009) A unifying model for the selective regulation of inducible transcription by CpG islands and nucleosome remodeling. *Cell* **138,** 114–128

nature COMMUNICATIONS

OPEN

ARTICLE

Received 12 Apr 2012 | Accepted 27 Jul 2012 | Published 4 Sep 2012

DOI: 10.1038/ncomms2023

Extracellular ATP mediates mast cell-dependent intestinal inflammation through P2X7 purinoceptors

Yosuke Kurashima[1,2,3], Takeaki Amiya[1,3,4], Tomonori Nochi[1], Kumiko Fujisawa[1,3], Takeshi Haraguchi[5], Hideo Iba[5], Hiroko Tsutsui[6], Shintaro Sato[1,3], Sachiko Nakajima[7], Hideki Iijima[7], Masato Kubo[8,9], Jun Kunisawa[1,4] & Hiroshi Kiyono[1,2,3,4]

Mast cells are known effector cells in allergic and inflammatory diseases, but their precise roles in intestinal inflammation remain unknown. Here we show that activation of mast cells in intestinal inflammation is mediated by ATP-reactive P2X7 purinoceptors. We find an increase in the numbers of mast cells expressing P2X7 purinoceptors in the colons of mice with colitis and of patients with Crohn's disease. Treatment of mice with a P2X7 purinoceptor-specific antibody inhibits mast cell activation and subsequent intestinal inflammation. Similarly, intestinal inflammation is ameliorated in mast cell-deficient $Kit^{W\text{-}sh/W\text{-}sh}$ mice, and reconstitution with wild-type, but not $P2x7^{-/-}$ mast cells results in susceptibility to inflammation. ATP-P2X7 purinoceptor-mediated activation of mast cells not only induces inflammatory cytokines, but also chemokines and leukotrienes, to recruit neutrophils and subsequently exacerbate intestinal inflammation. These findings reveal the role of P2X7 purinoceptor-mediated mast cell activation in both the initiation and exacerbation of intestinal inflammation.

[1] Division of Mucosal Immunology, Department of Microbiology and Immunology, The Institute of Medical Science, The University of Tokyo, 108-8639, Japan. [2] Graduate School of Medicine, The University of Tokyo, 113-0033, Japan. [3] Core Research for Evolutional Science and Technology (CREST), Japan Science and Technology Agency (JST), Tokyo 102-0075, Japan. [4] Department of Medical Genome Science, Graduate School of Frontier Science, The University of Tokyo, Chiba 277-8561, Japan. [5] Division of Host-Parasite Interaction, Department of Microbiology and Immunology, The Institute of Medical Science, The University of Tokyo, 108-8639, Japan. [6] Department of Microbiology, Hyogo College of Medicine, Nishinomiya 663-8501, Japan. [7] Department of Gastroenterology and Hepatology, Osaka University Graduate School of Medicine, 565-0871, Japan. [8] Research Center for Allergy and Immunology, RIKEN, Yokohama Institute, Tsurumi, Yokohama, Kanagawa, 230-0045, Japan. [9] Division of Molecular Pathology, Research Institute for Biological Sciences, Tokyo University of Sciences, Chiba 278-0022, Japan. Correspondence and requests for materials should be addressed to J.K. (email: kunisawa@ims.u-tokyo.ac.jp) or to H.K. (email: kiyono@ims.u-tokyo.ac.jp).

Both active and quiescent immunity occur simultaneously to achieve immunological homoeostasis in the harshest of environments—namely, the intestine. Aberrant immune responses in the gut lead to the development of intestinal immune diseases such as colitis and food allergies[1,2]. Mast cells (MCs) are generally recognized as major effector cells of type 1 allergic diseases, as well as of inflammation, host defenses, innate and adaptive immune responses and homoeostatic responses[3–5]. Histological analyses of patients with, and murine models of, colitis have implicated the involvement of MCs in intestinal inflammation[4,6], but the factors responsible for MC activation are not fully understood.

Several lines of evidence have demonstrated that release of extracellular ATP and ADP from injured, dying or activated cells acts as a danger signal by modulating various cellular functions via the activation of P2 purinoceptors[7,8]. P2 purinoceptors comprise P2X ($P2X_{1-7}$) and P2Y receptors ($P2Y_{1, 2, 4, 6, 11-14}$). $P2X_{1-7}$ receptors are ATP-gated ion channels and specific for ATP, whereas P2Y receptors are G protein-coupled receptors that are specific for ADP, UTP and ATP[7,8].

Stimulation by ATP or ADP through the P2 purinoceptors of macrophages and dendritic cells (DCs) results in the production of inflammatory cytokines; this can lead to the development of asthma, contact hypersensitivity or graft-versus-host disease[9–11]. MCs also express several P2 purinoceptors and release histamine, cytokines and chemokines upon nucleotide stimulation[12]. Although MCs are thought to be involved in intestinal inflammation, it is unclear whether extracellular nucleotides are required for this process.

Here, we used a newly established anti-MC monoclonal antibody (mAb) to identify activated MCs and found that extracellular ATP mediates MC activation through P2X7 purinoceptors to initiate and amplify intestinal inflammation. Consequently, obstruction of the ATP-P2X7 purinoceptor cascade could be used to inhibit gut inflammatory diseases.

Results

Activated MCs in intestinal inflammation. Using a 2,4,6-trinitrobenzene sulphonic acid (TNBS)-induced colitis model, we first examined whether MCs were involved in intestinal inflammation. To assess MC activation *in vivo*, we established an mAb (clone: 5A9) specific for CD63, a marker of activated MCs[13]. We confirmed that our anti-CD63 mAb was reactive specifically to MCs activated by immunoglobulin (Ig)E plus relevant allergen or a calcium ionophore, and not to naïve and CD63-knocked down MCs (Supplementary Fig. S1). In the colons of TNBS-treated mice, increased numbers of $CD63^+$-activated MCs were noted until day 3 post administration; the numbers then gradually decreased and reached a basal level on day 6 (Fig. 1a,b), indicating that MC activation was associated with the initiation phase of colitis development, as previously reported in a murine model and in patients with inflammatory bowel disease[6,14]. It has generally been accepted that the mechanistic basis of ulcerative colitis (UC) and Crohn's disease (CD) are different. Indeed, the pathogenic cytokines involved in the development of UC and CD are different[2] and the genetic polymorphisms specific for UC and CD are also different[15]. In addition, the cytokines required for the development of MCs differ between humans (stem cell factor) and mice [interleukin (IL)-3 and stem cell factor][4]. Thus, these different pathological environments may have led to differences in the requirement for, and involvement of, MCs in the development of inflammation. Therefore, we analysed MC numbers in both UD and CD patients, although we focused on the TNBS-induced colonic inflammation model. We detected increased numbers of MCs in the colons of patients with CD or UC (Fig. 1c,d). Thus, increased numbers of MCs in the colon is a characteristic of intestinal inflammation.

To directly show the involvement of MCs in the development of intestinal inflammation, we used MC-deficient $Kit^{W\text{-}sh/W\text{-}sh}$ mice. We confirmed that immunological and inflammatory symptoms induced by TNBS treatment were identical in $Kit^{W\text{-}sh/+}$ heterozygous and $Kit^{+/+}$ homozygous mice; however, inflammatory symptoms, such as body weight loss, massive inflammatory cell infiltration and colon shortening, were restored in $Kit^{W\text{-}sh/W\text{-}sh}$ mice but not in $Kit^{W\text{-}sh/+}$ heterozygous and $Kit^{+/+}$ homozygous mice (Fig. 1e–h). Similarly, our histological and immunological analyses revealed that destruction of the colonic epithelial layer and infiltration by inflammatory cells—especially neutrophils, which were stained neutral pink and had lobulated nuclei,—were reduced in $Kit^{W\text{-}sh/W\text{-}sh}$ mice (Fig. 1f,h,i). Moreover, inflammatory signs were ameliorated in $Kit^{W\text{-}sh/W\text{-}sh}$ mice when we used other well-known inflammatory bowel disease models, such as the dextran sodium sulphate (DSS) colitis model (Fig. 2a–c). As the use of $Kit^{W\text{-}sh/W\text{-}sh}$ mice as an MC-deficient model is controversial[16,17], we also used the MC-specific enhancer-mediated toxin receptor-mediated conditional cell knockout (TRECK) system (Mas-TRECK mice)[18]. We confirmed that specific depletion of MCs ameliorated the inflammation in this DSS-induced colitis model (Fig. 2d–h). Our data indicate that activated MCs participate in the aggravation of intestinal inflammation.

Establishment of an inhibitory MC-specific mAb. IgE plus a relevant allergen induces MC activation; however, $Rag\text{-}1^{-/-}$ and $Tcr\beta^{-/-}\delta^{-/-}$ mice showed inflammatory responses comparable to those in TNBS-induced intestinal inflammation (Supplementary Fig. S2a–d)[19] and had increased numbers of $CD63^+$-activated MCs in their colons (Supplementary Fig. S2e), suggesting that T and B cells are not involved in MC activation during colitis. We also found no increase in CD63 expression on MCs after stimulation with IL-18 and IL-33, which are known to be involved in colitis (Supplementary Fig. S2f)[20,21].

We next tried to establish an anti-MC mAb that could ameliorate activated MC-mediated intestinal inflammation. We immunized rats with purified murine-activated colonic MCs, established hybridomas, performed flow cytometry to select hybridomas that produced mAbs that preferentially recognized colonic MCs and examined the hybridomas' ability to inhibit ovalbumin-induced food allergy[22] or TNBS-induced intestinal inflammation (Supplementary Fig. S3). Among 2,000 clones, we obtained an anti-MC mAb (designated clone 1F11; rat IgG2b) that was strongly reactive to colonic MCs (Fig. 3a; Supplementary Fig. S3). In addition to colonic MCs, 1F11 mAb bound efficiently to peritoneal cavity-, lung- and bone marrow (BM)-derived MCs, but not to skin MCs (Fig. 3a). When tested with other immunocompetent cells in the colon, 1F11 mAb was weakly reactive to some $CD3^+$ T cells, $CD11c^+$ DCs and $F4/80^+$ macrophages, but was not reactive to $Gr\text{-}1^+$ granulocytes, IgA^+ plasma cells or epithelial cells (ECs) (Fig. 3b).

To show the inhibitory function of 1F11 mAb in intestinal inflammation, mice were given 1F11 mAb (0.5 mg day^{-1} in a single dose) for 3 days, beginning 1 day before intrarectal administration of TNBS. 1F11 mAb treatment reduced the intestinal inflammation (Fig. 3c–g) and decreased the number of $CD63^+$-activated MCs in 1F11 mAb-treated mice (Fig. 3h).

Targeting P2X7 receptors reduces intestinal inflammation. Mass spectrometry analyses of immunoprecipitants of MC cell lysates with 1F11 mAb showed that the P2X7 purinoceptor is recognized by 1F11 mAb (Supplementary Fig. S4a). The specificity of 1F11 mAb for the P2X7 purinoceptor was confirmed by its specific reactivity to cells transfected with P2X7 receptors but not with other types of P2X receptor (for example, P2X1 and P2X4; Supplementary Fig. S4b). MCs derived from $P2x7^{-/-}$ mice, however, were not recognized by 1F11 mAb (Supplementary Fig. S4c). Western blot and flow cytometric analysis showed that, among the several variants of P2X7 purinoceptors[23], 1F11 mAb bound to variant a (full-length; Supplementary Fig. S4d,e). In contrast, variant c (possessing